CNOIDAL WAVE FORMATION IN A LASER SYSTEM WITH ACTIVE SATURABLE ABSORBER

By:

Mario César Wilson Herrán, M. S.

Dissertation presented in partial fulfillment

of the requirements for the degree of

Doctor of Philosophy

in

Optics

Advisor

Dr. Vicente Aboites

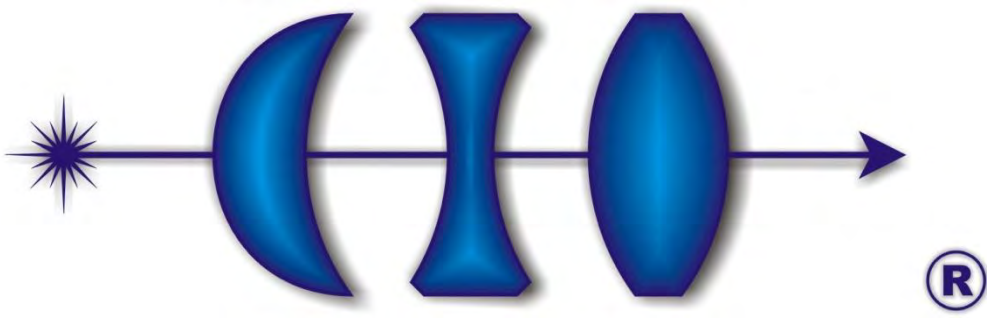

León, Gto. México

August 2011

Final version.
“Include all the suggestions and comments made by the thesis reviewers”

_____

Dr. Vicente Aboites
Thesis supervisor
León, Gto. August 22, 2011

ABSTRACT

We demonstrate the cnoidal wave formation in a two-laser system with a saturable absorber inside the cavity of one of the lasers. The other laser is used to activate the saturable absorber in order to control the pulse shape, width, intensity and frequency. The direct modulation enables to control when and how the pulse train coming from the saturable absorber is released. Using a three-level laser model rate equations based on the Statz – de Mars model, we show that for any value of saturable absorber parameter there exist a certain modulation frequency for which the pulse shape is very close to a soliton shape with less than 5% error at the pulse base. Such a device may be prominent for optical communication and laser engineering applications.

RESUMEN

Demostramos la formación de ondas cnoidales en un sistema de dos láseres con un absorbedor saturable dentro de la cavidad de uno de ellos. El otro láser es utilizado para activar al absorbedor saturable y así poder controlar la forma, el ancho, la intensidad y la frecuencia de los pulsos generados. La modulación directa permite controlar cuándo y cómo se libera el tren de pulsos que proviene del absorbedor saturable. Usando un modelo de ecuaciones de balance para un láser de tres niveles basados en el modelo de Statz – de Mars, demostramos que para cualquier valor de parámetro del absorbedor saturable existe cierta frecuencia de modulación con la que la forma del pulso generado es muy cercana a la forma de un solitón con menos del 5% de error en la base del pulso. Dicho dispositivo puede ser prominente para comunicaciones ópticas y aplicaciones de ingeniería láser.

To my Family. . .

ACKNOWLEDGMENTS

I would like to thank Dr. Vicente Aboites for his patience, support and encouragement in my research. I greatly appreciate the latitude I was given in pursuing the research contained in this dissertation. The lessons I learned in the approach to research will serve me well during the rest of my research career.

I would also like to thank Dr. Alexander Pisarchik for countless discussions which helped inspire the work contained in this thesis. His help in organizing my thoughts on solitons and dynamics is specially appreciated.

I would like to thank the other members of my committee, Dr. Bernardo Mendoza, Dr. Flavio Ruiz-Oliveras, Dr. Victor Pinto, Dr. Rider Jaimes-Reategui and Dr. Ismael Torres. Likewise, I especially remember Dr. Mendoza for his great comments on the Lyapunov seminar.

Furthermore, I want to thank Dr. Majid Taki and Dr. Saliya Coulibaly, for all the knowledge, patience and good moments in Lille, France.

I thank to all the people that directly or indirectly have something to do with this work, to the project No. M08P02 between ANUIES CONACyT – ECOS for providing me the opportunity to make two short stays in Lille, France, to the Instituto Euroamericano for the logistic support in some congresses and, especially, to the CONACyT for giving me financial support through the grant No. 174725.

I want to also thank my family as well as all my friends for their support in this quest. Thanks to my mother and father for helping me and motivating me to make it to where I am today.

Finally, I would like to thank my wife Linda. She has stood by me through all these years of my doctoral study with love, patience, support and great friendship. I will always cherish these years during which we grew together and fell in love. Thank you.

MARIO CÉSAR WILSON HERRÁN

Centro de Investigaciones en Óptica, A.C.

August 2011

CONTENT

INDEX……..……..…V

FIGURES LIST……..…….……..VIII

THESIS GENERAL OVERVIEW…….……..……XI

CHAPTER 1

PRELIMINARIES

1.0 INTRODUCTION..……..….....1

1.1 SOLITONS……..……..…….……..…1

1.2 ELLIPTIC FUNCTIONS……...7

1.3 CNOIDAL WAVE…..……..…….…..9

1.4 RATE EQUATIONS…….……11

1.4.1 RATE EQUATIONS IN ABSENCE OF AMPLIFIER RADIATION.....13

1.4.2 RATE EQUATIONS IN PRESENCE OF AMPLIFIER RADIATION…...14

1.5 STATZ – DE MARS MODEL…….....15

1.6 SATURABLE ABSORBERS……...17

FIRST CHAPTER REFERENCES……..18

CHAPTER 2

THEORETICAL MODEL

2.0 INTRODUCTION…….…….....20

2.1 LASER SCHEME…….20

2.2. LASER MODEL……...21

2.3 LINEAR STABILITY ANALYSIS…….....27

SECOND CHAPTER REFERENCES…….32

CHAPTER 3

RESULTS AND CONCLUSIONS

3.0 INTRODUCTION…….34

3.1 CONTROLLING THE SYSTEM DYNAMICS……...34

3.2 CNOIDAL WAVE OBSERVATION……...40

3.3 CONCLUSIONS……...44

3.4 FUTURE WORK……..……45

THIRD CHAPTER REFERENCES…….47

APPENDIX 1

LIST OF PUBLICATIONS

A1.1 PEER-REVIEWED INDEXED JOURNALS……..i

A1.2 CONFERENCES……ii

FIGURES LIST

CHAPTER 1 PRELIMINARIES

Figure 1 Russell's scheme of his studies about the "wave of translation"

Figure 2 A solitary wave travelling to the beach in a Hawaiian isle.

Figure 3 Light bullets interaction, when these type of soliton interact they lose certain quantity of energy.

Figure 4 Argand diagram constructed to show the formation of the Jacobi elliptic functions

Figure 5 Cnoidal wave profile achieve for different parameter's value.

Figure 6 Cnoidal wave limits. a)sinusoidal shape. b) soliton shape.

Figure 7 Two energy levels diagram including life-times

Figure 8 Energy levels 1 and 2 with surrounding higher and lower energy levels

Figure 9 The population densities N_1 and N_2 ($cm^{-3}s^{-1}$) of atoms in energy levels 1 and 2 are determined by three processes: decay (b), pumping(r), and absorption and stimulated emission (g)

CHAPTER 2 THEORETICAL MODEL

Figure 10 Optical scheme for a laser system with an active saturable absorber. *AM* and *SA* are active medium and saturable absorber, M_1 and M_2 are total reflected and semi-transparent laser mirrors, and *EOM* is an electro-optical modulator.

Figure 11 A laser cavity with an active medium and a saturable absorber.

Figure 12 Stability condition given by the relation between α and α_α.

CHAPTER 3 RESULTS AND CONCLUSIONS

Figure 13 Laser output without external modulation, the system tends to a fixed point.

Figure 14 Laser output with fixed modulation (ω = 1) and variable absorption ratio. a) α_α = 0.3, b) α_α = 1, c) α_α = 3, d) α_α = 15, e) α_α = 30 and f) α_α = 60.

Figure 15 Phase diagram *m* vs n_a. a) with α_a = 1.4 b)with α_a = 30.

Figure 16 Pulse shape at α_a = 15 with different frequencies a) ω = 1/4, b) ω = 1/2, c) ω = 2, d) ω = 5, e) ω = 10, f) ω = 35.

Figure 17 Pulse width against control frequency. It is shown how the pulses width become narrower as the control frequency is increased.

Figure 18 Laser output intensity for α_a = 15 and control frequencies (a) ω = 1, (b) 5, (c) 15, (d) 25, (e) 50, and (f) 75.

Figure 19 Overlapping of one pulse taken at α_a = 15 and ω = 25 (solid line) with a $sech^2$ wave form (dashed line).

Figure 20 Modulation frequency ω_s and absorption ratio of saturable absorber corresponding to soliton-shape pulses.

Figure 21 Experimental set-up implemented for search cnoidal waves.

Figure 22 Experimental cnoidal wave limits. a) soliton-shape limit, b) sinusoidal shape limit.

THESIS GENERAL OVERVIEW

This thesis presents the study of a laser with an active saturable absorber by means of the rate equations; the main objective is to produce cnoidal waves through controlling the laser dynamics.

The thesis is composed by three chapters that are organized as follows

Chapter 1: Preliminaries

In this chapter the elemental concepts needed to have a better understanding of the work are boarded. The chapter contemplates subjects as solitons, elliptic functions, rate equations, cnoidal waves and saturable absorbers.

Chapter 2: Theoretical model

In this chapter, the experiment proposal is presented, with the aid of the rate equations. A model for the experiment is proposed and its linear stability analysis is done in order to know the fixed points of the system and its stability.

Chapter 3: Results and conclusions

In this part of the thesis, the obtained results are presented; the chapter contains the dynamics control and the cnoidal waves observation. At the end of the

chapter, the conclusions are followed by a future work proposal (some preliminaries results have been obtained).

As an appendix there is a list of publications made during the doctoral studies.

CHAPTER 1

PRELIMINARIES

1.0.INTRODUCTION

In this chapter a basic introduction to the matters dealt in this dissertation are presented in order to have a better understanding of the results discussed in this dissertation.

1.1. SOLITONS

The first natural definition that comes to mind when the word ***soliton*** is heard reefers to a self-reinforcing solitary wave that does not have variation on its shape while it is traveling along a media at a constant speed.

These kinds of waves are caused by compensation (cancellation) between the nonlinear (e.g. Kerr and Raman effects in fiber optics) and the dispersive effects of the propagating medium. Solitons exist as a solution of many weakly nonlinear dispersive partial differential equations, used to describe different physical phenomena [1].

In 1844, John Scott Russell reported the observation of a solitary wave [2] in the Union Canal, Scotland, while he was doing some experiments to determine the most efficient design for canal boats. He called that phenomenon wave of translation, and by his own words it was described as follows:

> I was observing the motion of a boat which was rapidly drawn along a narrow channel by a pair of horses, when the boat suddenly stopped—not so the mass of water in the channel which it had put in motion; it accumulated round the prow of the vessel in a state of violent agitation, then suddenly leaving it behind, rolled forward with great velocity, assuming the form of a large solitary elevation, a rounded, smooth and well-defined heap of water, which continued its course along the channel apparently without change of form or diminution of speed. I followed it on horseback, and overtook it still rolling on at a rate of some eight or nine miles an hour [14 km/h], preserving its original figure some thirty feet [9 m] long and a foot to a foot and a half [300−450 mm] in height. Its height gradually diminished, and after a chase of one or two miles [2–3 km] I lost it in the windings of the channel. Such, in the month of August 1834, was my first chance interview with that singular and beautiful phenomenon which I have called the Wave of Translation."

Russell spent a lot of time trying to repeat and understand these kinds of waves (see Fig. 1); after several tries he found some properties:

- The waves are stable in long distances.
- The speed depends on the wave's amplitude and the wave's width on the deepness of the water.
- They never merge between them.
- If the medium can't contain a big wave due the water depth, the wave splits into two, one bigger than the other.

Despite of Russell's founds, the scientific community didn't accept his discoveries due to the contrast with the Newton and Bernoulli theories of hydrodynamics.

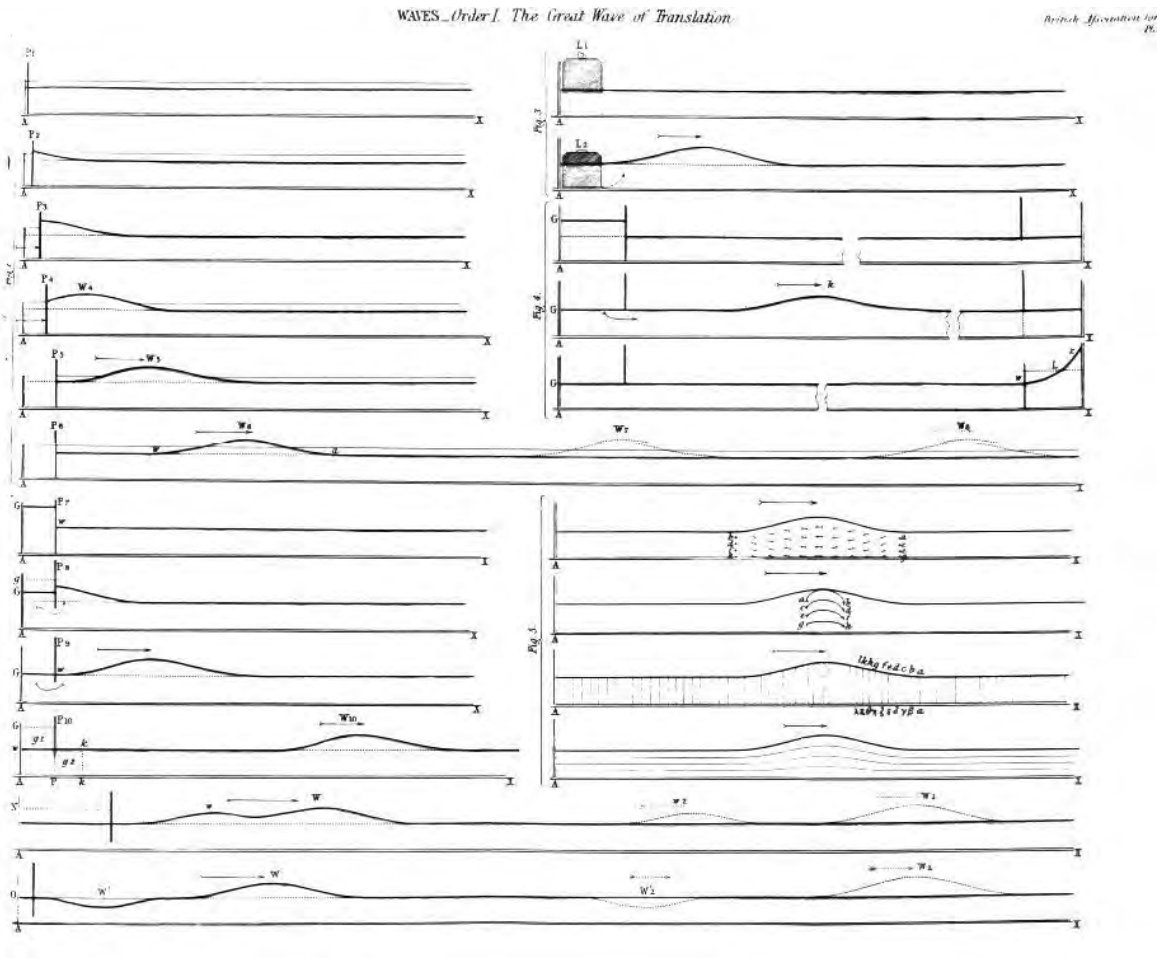

FIGURE 1. Russell's scheme of his studies about the "wave of translation"

The problem was theoretically unexplained until 1876, when Lord Rayleigh published a paper in the "Philosophical Magazine" supporting Russell's experimental observation. In that paper, Lord Rayleigh presented his mathematical theory [3] and mentioned that the first theoretical treatment was made by Joseph Boussinesq five years earlier [4] (Boussinesq also cited Russell in his work). Twenty years later, Korteweg and de Vries published a paper called "On the change of form of long waves advancing in a rectangular canal and on a new type of long stationary waves" also in the

–Philosophical Magazine" [5], in this work they didn't mentioned John Russell, but they did quote Boussinesq and Rayleigh papers. This work is one of the milestones in the construction of the modern soliton theory.

The equation presented by Korteweg - de Vries (KdV) is:

$$u_t + \alpha u u_x + \beta u_{xxx} = 0, \tag{1}$$

where: α and β are constants and $u(x,t)$ represents the amplitude from the average water surface and x is the coordinate moving with linearized wave velocity. Equation (1) has a solitary wave (Fig. 2) solution:

$$u(x,t) = \frac{3v}{\alpha}\sec h^2\left[\frac{1}{2}\sqrt{\frac{v}{\beta}}(x - vt)\right]. \tag{2}$$

FIGURE 2. A solitary wave travelling to the beach in a Hawaiian isle.

In 1955 Fermi and its colleagues [6] investigated how the equilibrium state is approached in a one dimensional nonlinear lattice. The researchers expected that the non-linear interactions among the normal modes of the linear system would lead to the energy of the system being evenly distributed throughout all modes; that is, an ergodic system. Amazingly, the results contradicted these ideas. The energy was not uniformly distributed in all modes, but, after some time, the system returned to its original state. Ten years later, Zabusky and Krustal [7] solved the KdV equation as a model for a non-linear lattice and observed the same phenomenon that Fermi reported before [6] and they observed that, with a smooth initial waveform, waves with sharp peaks emerge. Those pulse-waves moved almost independently with constant speeds and passed through each other without distortions after collisions. They performed a detailed analysis about these waves and found that each pulse was a solitary wave of sech^2-type (the KdV solitary wave solution) and also that the waves behaved like stable particles.

Equation (1) can be rewritten as:

$$u_t - 6uu_{xx} + u_{xxx} = 0. \tag{3}$$

In this form, the second and third terms represent the nonlinear and dispersion effects respectively [8]. The dispersion effects makes a wave spread while the nonlinear effect causes the steepening of the waveform, if these two effects are compensated a soliton could exist.

As can be seen, it is not easy to give a comprehensive and precise definition of a soliton. However, the term shall be associated with any solution of a non-linear system (or equation) which fulfills the following characteristics:

- Represents a wave with constant shape (sech or $sech^2$).
- It's localised in a region (it decays at infinity).
- Can interact strongly with other solitons without losing energy.

Some scientists use the term soliton when they are working with solutions that fulfills the first two characteristics [9-10] (e.g. Light Bullets are called solitons, despite losing energy when they interact, Fig. 3).

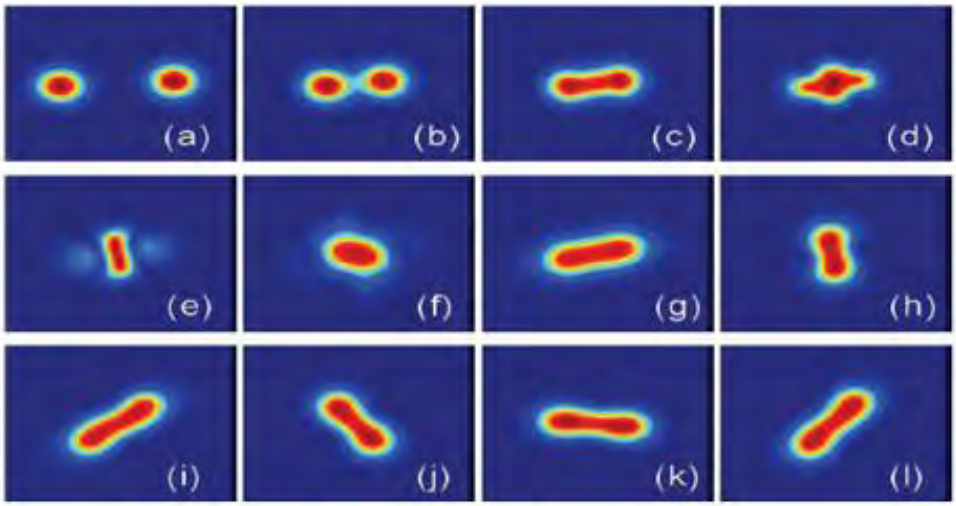

FIGURE 3. Light bullets interaction, when these type of soliton interact they lose certain quantity of energy.

1.2. ELLIPTIC FUNCTIONS

An elliptic function is a function defined in the complex plane that is periodic in two directions and, at the same time, is meromorphic [11]. These functions were discovered as inverse functions of elliptic integrals, hence the name derives.

Elliptic functions are important to have a better understanding of solitons due to its characteristics.

Defining the next integral as:

$$v = \int_0^{\phi} \frac{d\theta}{\left(1 - m\sin^2\theta\right)^{1/2}}, \tag{4}$$

where *m*, the parameter, is restricted to $0 \le m \le 1$. Equation (4) can be compared with the elementary integral:

$$w = \int_0^{\psi} \frac{dt}{\left(1 - t^2\right)^{1/2}} \tag{5}$$

where $t = \sin\theta$ so that $w = \arcsin\psi$ or $\sin w = \psi$, and so observe that Eq. (5) defines the inverse of the trigonometric function, sin. This relation led the mathematician Carl Jacobi to define a new pair of inverse functions from Eq. (4)

$$\begin{aligned} \operatorname{sn} v &= \sin\phi, \\ \operatorname{cn} v &= \cos\phi. \end{aligned} \tag{6}$$

These are two of the twelve Jacobian elliptic functions (those functions can be constructed with the aid of the Argand diagram shown in Fig. 4) and are normally written as sn($v|m$) and cn($v|m$). To denote the parameter dependence (it is usual also to work with the modulus, k, where $m = k^2$ [12].

The two special cases for $m = 0,1$ enable Eqs. (4) and (6) to be reduced to elementary functions: if $m = 0$ then, $v = \phi$ and so cn($v|0$) = cos ϕ = cos v, and if $m = 1$ the integral can be evaluated to yield $v = \text{arcsech}(\cos\phi)$ and so cn($v|1$) = sech v. It therefore follows that cn($v|m$) and sn($v|m$) are periodic functions for $0 \le m < 1$, but that periodicity is lost for $m = 1$. Now the period of cn and sn corresponds to the period 2π of cos and sin, and so the period of these elliptic functions can be written as:

$$\int_0^{2\pi} \frac{d\theta}{\left(1 - m\sin^2\theta\right)^{1/2}} = 4\int_0^{\pi/2} \frac{d\theta}{\left(1 - m\sin^2\theta\right)^{1/2}} \tag{7}$$

This latter integral is the complete elliptic integral of the first kind (because it's bounded),

$$K(m) = \int_0^{\pi/2} \frac{d\theta}{\left(1 - m\sin^2\theta\right)^{1/2}}. \tag{8}$$

It is obvious that $K(0) = \pi/2$, and it is also straightforward to show that $K(m)$ increases monotonically as m increases. In fact $K(m) \sim \frac{1}{2}\log\left[16/(1-m)\right]$ as $m \to 1^-$, and so

$K(m) \to +\infty$ as $m \to 1^-$, this demonstrate the infinite period of the cn(v|1) = sech v function.

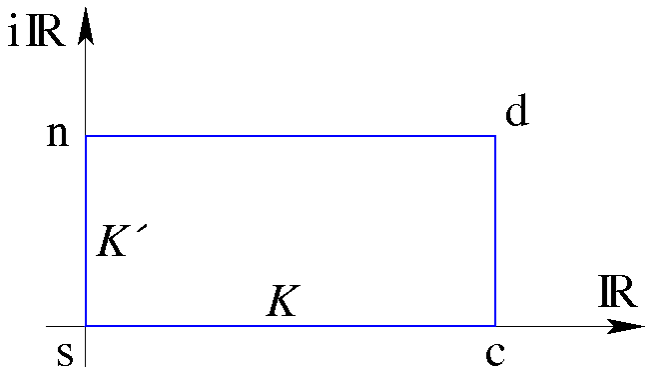

FIGURE 4. Argand diagram constructed to show the formation of the Jacobi elliptic functions

1.3. CNOIDAL WAVE

Another important contribution of Korteweg-de Vries was the cnoidal wave. The cnoidal wave is an exact non-linear periodic solution to the KdV equation [5]. These solutions are described in terms of the Jacobi elliptic function cn, hence their name came from.

The main characteristic of these waves is that they are parametrically bounded by the parameter (i.e. ellipticity); they change their shape from a sinusoidal (when the ellipticity is zero) to a soliton-like (when the ellipticity tends to one) as shown in Fig. 5.

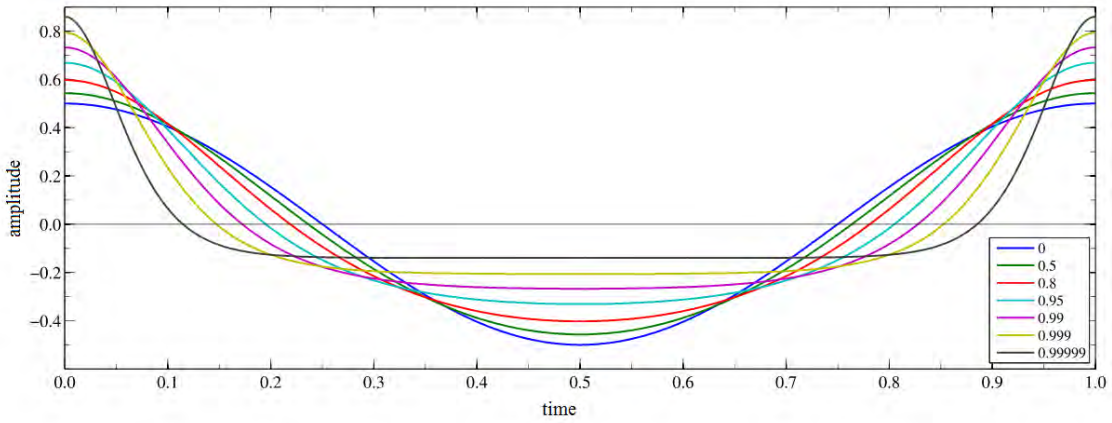

FIGURE 5. Cnoidal wave profile achieved for different parameter's value.

These waves are not exclusive for the KdV equation; they can be found in any system able to produce solitons (e.g. Boussinesq equations, non-linear Schrödinger equation, shallow water equations, Sine-Gordon equation) [1-13].

The amplitude $A(x,t)$ as a function of the horizontal position, x, and time, t, for a cnoidal wave is given by:

$$A(x,t) = A_2 + H\,\mathrm{cn}^2\left(2K(m)\frac{x-ct}{\lambda}\,|\,m\right) \tag{9}$$

where A_2 is the trough elevation, H is the wave height, c is the phase speed and λ is the wavelength. Further cn correspond to one of the Jacobi elliptic functions and $K(m)$ is the complete elliptic integral of the first kind; both depend on the elliptic parameter m. This parameter determines the cnoidal wave shape; for $m = 0$ the cnoidal wave becomes a cosine function, while for $m \to 1$ the cnoidal wave is transformed into a hyperbolic secant function, as is illustrated in Fig. 6.

Cnoidal waves (also found as soliton trains) have been a hot research topic in lasers over the past 15 years; the published articles are basically about cnoidal wave stability, formation in quadratic and cubic media, techniques to stabilize the cnoidal trains and generation of cnoidal wave in passive q-switched and mode-locked fiber laser [14-17].

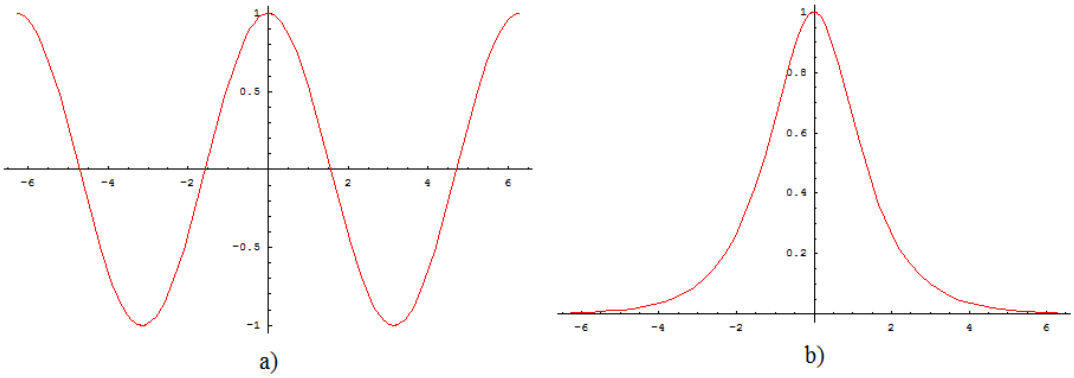

FIGURE 6. Cnoidal wave limits. a)sinusoidal shape. b) soliton shape.

1.4. RATE EQUATIONS

To lase, an inverted population level must be achieved and maintained in a laser media. For laser operation, excitation and decay rates of all of the different energy levels participating in the process must be balanced to maintain a steady-state inverted population for the radiative transition [18-19]. The equations describing the change rates of the population densities N_1 and N_2 as a result of pumping, radiative, and non-radiative transitions are called the rate equations.

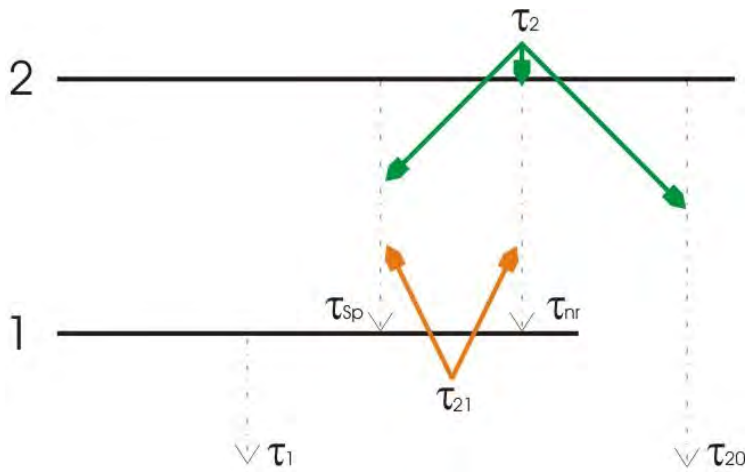

FIGURE 7. Two energy levels diagram including life-times

Consider the energy diagram of Fig. 7. Levels 1 and 2 have overall life-times τ_1 and τ_2, respectively, permitting transitions to lower levels. The lifetime of level 2 has two contributions: one associated with decay from 2 to 1 (τ_{21}), and the other (τ_{20}) associated with decay from 2 to all other lower levels. When several modes of decay are possible, the overall transition rate is a sum of the component transition rates. Since the rates are inversely proportional to the decay times, the reciprocals of the decay times must be added as $\tau_2^{-1} = \tau_{21}^{-1} + \tau_{20}^{-1}$. Multiple modes of decay therefore shorten the overall life-time. Aside from the radiative spontaneous emission component (with time constant τ_{sp}) in τ_{21}, a non-radiative contribution, τ_{nr}, may also be present, so that $\tau_{21}^{-1} = \tau_{sp}^{-1} + \tau_{nr}^{-1}$.

If a system like the illustrated in Fig. 7 is allowed to reach the steady-state, the population densities N_1 and N_2 will vanish by virtue of all the electrons ultimately decaying to lower levels.

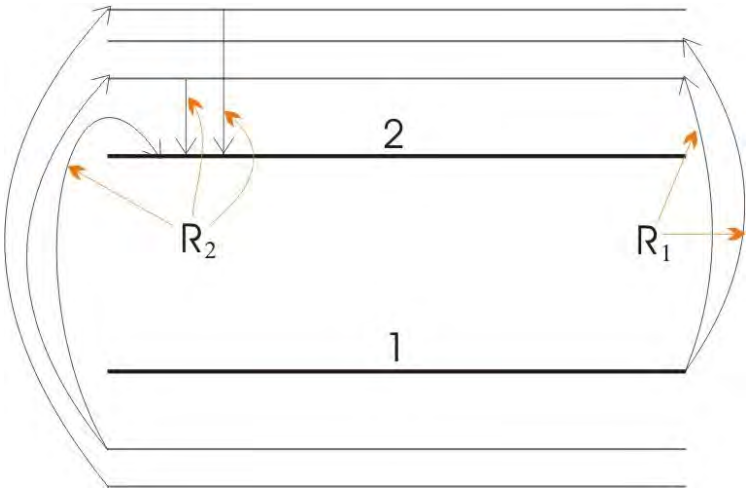

FIGURE 8. Energy levels 1 and 2 with surrounding higher and lower energy levels

Steady-state populations of levels 1 and 2 can be maintained, however, if energy levels above level 2 are continuously excited and leak downward into level 2, as shown in the more realistic energy level diagram of Fig. 8. Pumping can bring atoms from levels other than 1 and 2 out of level 1 and into level 2, at rates R_1 and R_2 (per unit volume per second), respectively. Consequently, levels 1 and 2 can achieve non-zero steady-state populations.

1.4.1. RATE EQUATIONS IN THE ABSENSE OF AMPLIFIER RADIATION

The population densities increase rate of levels 2 and 1 arising from pumping and decay are:

$$\begin{aligned} \frac{dN_2}{dt} &= R_2 - \frac{N_2}{\tau_2}, \\ \frac{dN_1}{dt} &= -R_1 - \frac{N_1}{\tau_1} + \frac{N_2}{\tau_{21}}. \end{aligned} \tag{10}$$

Under steady-state condition ($\dot{N}_1 = \dot{N}_2 = 0$), Eqs. (10) can be solved for N_1 and N_2 and the population difference $N_0 = N_2 - N_1$ can be found. The result is:

$$N_0 = R_2\tau_2\left(1-\frac{\tau_1}{\tau_{21}}\right)+R_1\tau_1. \tag{11}$$

1.4.2. RATE EQUATIONS IN THE PRESENCE OF AMPLIFIER RADIATION

The presence of radiation near the resonance frequency enables transitions between levels to take place by the processes of stimulated emission and absorption as well, characterized by the probability density W_i and shown in Fig. 9. The Eqs. (10) must be extended to include this source of population variation in each level

$$\begin{aligned}\frac{dN_2}{dt} &= R_2 - \frac{N_2}{\tau_2} - N_2W_i + N_1W_i,\\ \frac{dN_1}{dt} &= -R_1 - \frac{N_1}{\tau_1} + \frac{N_2}{\tau_{21}} + N_2W_i - N_1W_i.\end{aligned} \tag{12}$$

Under steady-state condition ($\dot{N}_1 = \dot{N}_2 = 0$) eqs. (12) can be solved for N_1 and N_2, thus, the population difference $N = N_2 - N_1$ is found.

$$\begin{aligned}N &= \frac{N_0}{1+\tau_sW_i} \text{ with}\\ \tau_s &= \tau_2 + \tau_1\left(1-\frac{\tau_2}{\tau_{21}}\right),\end{aligned} \tag{13}$$

where τ_s is the characteristic time which is always positive since $\tau_2 \le \tau_{21}$.

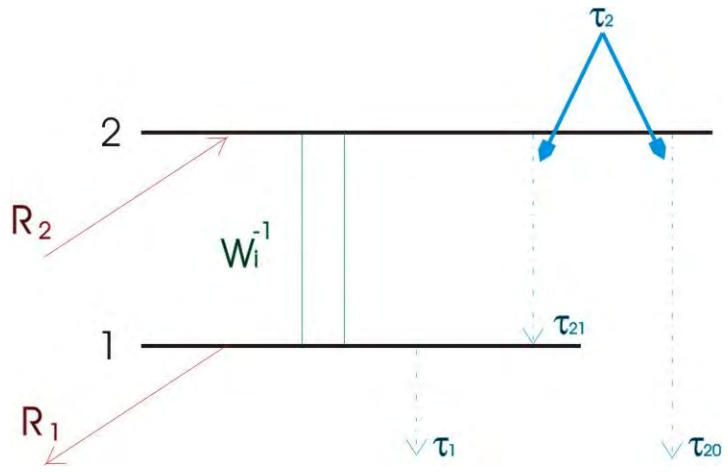

FIGURE 9. The population densities N_1 and N_2 ($cm^{-3}s^{-1}$) of atoms in energy levels 1 and 2 are determined by three processes: decay (b), pumping(r), and absorption and stimulated emission (g)

1.5. STATZ – DE MARS MODEL

The rate equations proposed by H. Statz and G. de Mars (SdM) are independent of the number of the laser's energy levels because are based in the phenomenology that leads the laser to emit stimulated radiation [20]. This characteristic allows to model different types of laser systems (e.g. dye, solid state, semiconductor, fiber). This model is given by the following set of equations:

$$\begin{aligned} \frac{dM}{dt} &= B'M(t)N(t) - \frac{M(t)}{T}, \\ \frac{dN}{dt} &= \beta B'M(t)N(t) + \frac{No - N(t)}{\tau}, \end{aligned} \tag{14}$$

where $N(t)$ represents the population inversion density and $M(t)$ the emitted photon density at a determinate frequency. The emitted photon density is directly linked with

the photon-flux density $S(t)$. If we divide the photon-flux between the propagation speed of light v and the photons energy $h\nu$ we obtain the emitted photons density; this is:

$$M(t) = \frac{S(t)}{vh\nu}. \tag{15}$$

The constant B' means $Bh\nu$, where B is the Einstein coefficient for stimulated transitions. T represents the photons life-time inside the resonant cavity, which is inversely proportional to the sum of the losses coefficients ξ_1 and ξ_2:

$$T = \frac{1}{v(\xi_1 + \xi_2)} \tag{16}$$

τ represents the relaxation time of the population inversion difference between levels where the laser emission takes place; β is a constant that depends of the level numbers of the system and N_0 stands for the equilibrium value of the population inversion density achieved in absence of laser oscillation.

The physical interpretation of the SdM equations is especially simple. The first equation states that the photons density grows as a consequence of the stimulated transitions inside the cavity and decreases due to losses imputable to the medium and the resonator [21]. The growth of the emitted photons density to a certain frequency is directly proportional to the product of the same emitted photons quantity at that frequency by the population inversion density of the laser medium. The second equation shows that

the population inversion density will decrease because of the stimulated emission and will grow due to the pumping action on the upper energy levels of the medium.

1.6. SATURABLE ABSORBERS

A saturable absorber (SA) is a non-linear optical component with a certain optical loss, which is reduced at high optical intensities [18]. SAs are usually used for passive mode-locking and Q-switching depending on their parameters. It is well known that continuous wave dye lasers with SAs provide short pulses due to self-stabilization of the pulse shaping process. A SA inserted into a laser cavity increases the nonlinearity of such system and enriches the laser operation dynamics. Mode-locking laser dynamics has been an important study subject, traditionally mode-locking is actively obtained with an optical modulator inside the cavity or passively with a SA.

The principal characteristics of a SA are: modulation depth (maximum possible change in optical loss), unsaturable losses (unwanted losses which cannot be saturated), recovery time, saturation fluence, saturation energy and damage threshold (given in terms of intensity) [22].

When dealing with pulses, a fast saturable absorber has a recovery time well below the pulse duration, while a slow absorber has it well above the pulse duration. The same device may be either a fast absorber or a slow absorber, depending on the pulses used with [19]. The saturation parameter of a saturable absorber is the ratio of the incident pulse fluence to the saturation fluence of the device.

FIRST CHAPTER REFERENCES

1. P. G. Drazin and R. S. Johnson, *Solitons: An introduction*. *2nd ed*. (Cambridge University Press, 1989).
2. J. S. Russell, "Report on waves", Fourteenth Meeting of the British Association for the Advancement of Science (1844).
3. Lord Rayleigh, "On waves", Phil. Mag. **1**, 257-279 (1876).
4. J. de Boussinesq "Théorie des ondes et des remous qui se propagent le long d'un canal rectangulaire horizontal en communiquant au liquide continu dans ce canal des vitesses sensiblement pareilles de la surface au fond", J. Math. Pures et Appliquées **2**, 55 (1872).
5. D. J. Korteweg and G. de Vries, "On the Change of Form of Long Waves advancing in a Rectangular Canal and on a New Type of Long Stationary Waves", Phil. Mag. **39,** 422–443 (1895).
6. E. Fermi, J. Pasta, and S. Ulam, "*Studies of Nonlinear Problems*", Document LA-1940 (May 1955).
7. N. J. Zabusky and M. D. Kruskal, "Interaction of 'Solitons' in a collisionless plasma and the recurrence of initial states", Phys. Rev. Lett. **15**, 240-243 (1965).
8. M. Wadati, "Introduction to solitons", Pramana J. Phys. **57**(5), 841-847 (2001).
9. N. Akhmediev and A. Ankiewicz, *Solitons Nonlinear Pulses and Beams* (Chapman & Hall, 1997).
10. G. P. Agrawal, *Optical solitons, autosolitons and similaritons.* (Institute of Optics, Rochester, NY, 2008).

11. N. I. Akhiezer, *Elements of the Theory of Elliptic Functions*, (AMS, Rhode Island, 1990).

12. M. Abramowitz and I. A. Stegun, *Handbook of Mathematical Functions with Formulas, Graphs, and Mathematical Tables*, (New York: Dover, 1965).

13. D. Powell, ―Rogue waves captured", ScienceNews **179**(13), 12 (2011).

14. C. Newell and J. V. Moloney, *Nonlinear Optics* (Addison-Wesley Publishing Co., 1992).

15. Y. Yang, *Solitons in field theory and nonlinear analysis*. (Springer-Verlag, 2001).

16. N. Manton and P. Sutcliffe, *Topological solitons* (Cambridge University Press, 2004).

17. Y. A. Kartashov, A. A. Egorov, A. S. Zelenina, V. A. Vysloukh and L. Torner, ―Stabilization of one-dimensional periodic waves by saturation of the nonlinear response", Phys. Rev. E **68**, 065605(R) (2003).

18. A. E. Siegman, *Lasers*, (University Science Books, 1986).

19. O. Svelto, *Principles of Lasers*, Fourth edition, (Springer, 1989).

20. H. Statz and G. De Mars, ―Transients and Oscillation Pulses in Masers", Quantum Electronics, 530-537 (1960).

21. L. Tarassov, *Physique des Processus dans les Générateurs de Rayonnement Optique Cohérent* (Éditons MIR, 1981).

22. H. Haken, *Laser Light Dynamics*, (North Holland Physics Publishing, 1985).

CHAPTER 2

THEORETICAL MODEL

2.0. INTRODUCTION

In this chapter the system configuration is presented, the modeling will be made and the stability analysis of the obtained model will be performed. The system dynamics will be discussed in order to find the best regions to control the system.

2.1. LASER SCHEME

The proposed configuration is composed by a laser made up with an active medium (AM), two mirrors (total reflexion, M1, and semitransparent, M2) and an intracavity saturable absorber (SA) coupled with a low-power continuous wave laser (CW) through an electro-optical modulator (EOM) as shown in Fig. (10)

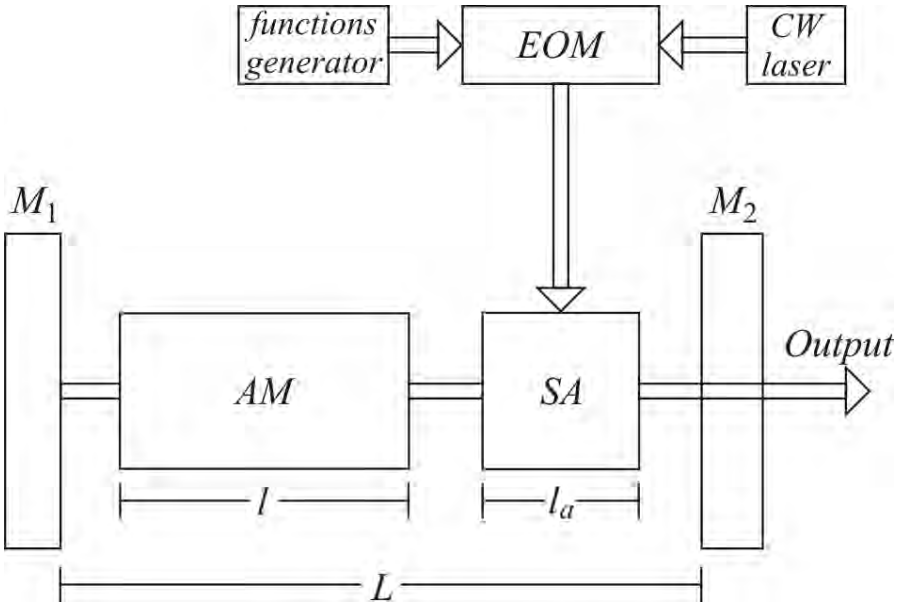

FIGURE 10. Optical scheme for a laser system with an active saturable absorber. *AM* and *SA* are active medium and saturable absorber, M_1 and M_2 are total reflected and semi-transparent laser mirrors, and *EOM* is an electro-optical modulator.

2.2. LASER MODEL

Is assumed that the proposed system is a three-level laser [1] obeying the following equations:

$$\begin{aligned} \frac{1}{v}\frac{dS(t)}{dt} &= \sigma N(t)S(t) - \left(\xi_1 + \xi_2\right)S(t), \\ \frac{dN(t)}{dt} &= -\frac{2\sigma}{h\omega}S(t)N(t) - \left(Z+1\right)\frac{n}{\tau}, \end{aligned} \tag{17}$$

where: $S(t)$ and $N(t)$ stands for the photon-flux density and the population inversion density inside the cavity, σ is the effective cross-section of interaction between active centers and photons; the coefficient for absorption and dispersion is represented by ξ_1

meanwhile the coefficient of the losses that depend on the mirrors reflectivity is ξ_2; v is the speed of light in the medium, τ represents the life-time between energy levels, n stands for the number of active centers per volume unit on the medium and $Z = W_p \tau$ where W_p represents the stimulated emission transition probability and finally $\hbar\omega$ is the photon energy.

The saturable absorber will be modeled by two-level active resonant centers [2,3], so that all the active absorbents centers are on a lower energy level to get the resonant photons to cause the maximum opacity. The rate equations that describe the active centers of the absorber are:

$$\begin{aligned} \frac{dn_{2\alpha}}{dt} &= B_\alpha n_{1\alpha} \frac{S}{v_\alpha} - B_\alpha n_{2\alpha} \frac{S}{v_\alpha} - \frac{n_{2\alpha}}{\tau_\alpha}, \\ \frac{dn_{1\alpha}}{dt} &= B_\alpha n_{2\alpha} \frac{S}{v_\alpha} - B_\alpha n_{1\alpha} \frac{S}{v_\alpha} - \frac{n_{2\alpha}}{\tau_\alpha}, \end{aligned} \tag{18}$$

where B_α is the Einstein coefficient for stimulated emission on the absorber, and $1 / \tau_\alpha$ is the probability of spontaneous emission for the absorbers active centers. Denoting by $n_{1\alpha}$ and $n_{2\alpha}$ the density of active centers of the absorber in the lower and upper energy levels, respectively, the total density of active centers of the absorber is given by $n_\alpha = n_{1\alpha} + n_{2\alpha}$ and then we have that in $t = 0$

$$\begin{aligned} n_{1\alpha} &= n_\alpha, \\ n_{2\alpha} &= 0. \end{aligned} \tag{19}$$

When enough power-pump is applied the saturation condition can be achieved

$$n_{1\alpha} = n_{2\alpha} = \frac{n_\alpha}{2}. \tag{20}$$

Population inversion density of the absorber is defined as $N_\alpha = n_{2\alpha} - n_{1\alpha}$, deducing from Eqs. (19) and (20):

$$\frac{dN_\alpha}{dt} = -\frac{2B_\alpha N_\alpha S}{v_\alpha} - \frac{\left(N_\alpha + n_\alpha\right)}{\tau_\alpha}. \tag{21}$$

Defining the absorption coefficient for the absorber as:

$$k_\alpha = -\sigma_\alpha N_\alpha, \tag{22}$$

where σ_α is the effective section of stimulated emission given by $\sigma_\alpha = \frac{\hbar\omega B_\alpha}{\mathrm{v}_\alpha}$, where v_α represents the speed of light on the absorber and ω is the angular frequency.

If we multiply Eq. (21) by $-\sigma_\alpha$, it can be rewritten as:

$$\frac{dk_\alpha}{dt} = -\frac{2B_\alpha k_\alpha S}{\mathrm{v}_\alpha} + \frac{\left(k_{0\alpha} - k_\alpha\right)}{\tau_\alpha}, \tag{23}$$

where $k_{0\alpha}$ is the initial absorption coefficient given by $k_{0\alpha} = -\sigma_\alpha N_\alpha(0) = \sigma_\alpha n_\alpha$.

Steady-state implies that $\frac{dk_\alpha}{dt} = 0$, and Eq. (23) becomes:

$$k_\alpha = \frac{k_{0\alpha}}{1 + \frac{S}{S_{\alpha_{Sat}}}}, \tag{24}$$

where $S_{\alpha_{Sat}}$ is the photon-flux in where the absorption coefficient k_α falls down to half its initial value $k_{0\alpha}$.

Being ξ_α the non-resonant absorption coefficient, K_α the total absorption coefficient of the absorber defined as: $K_\alpha = k_\alpha + \xi_\alpha$. Once this relation is satisfied, the photon flux average equation of the active medium may be expressed by:

$$S_{S_{at}} + \frac{L_m}{v}\frac{d\langle S\rangle}{dt} = L_m\sigma\langle N\rangle\langle S\rangle - L_m(\xi_1)\langle S\rangle, \tag{25}$$

where L_m is the active medium length.

The photon-flux average equation inside the absorber is given by:

$$\begin{aligned} &S_{S_{at}} + \left(\frac{L_m}{v} + \frac{L_\alpha}{v_\alpha} + \frac{L-(L_m+L_\alpha)}{c}\right)\frac{d\langle S\rangle}{dt} = \\ &L_m\sigma\langle N\rangle\langle S\rangle + L_\alpha\sigma_\alpha\langle N_\alpha\rangle\langle S\rangle - L_m\xi_l\langle S\rangle - L_\alpha\xi_\alpha\langle S\rangle \end{aligned} \tag{26}$$

And the filling-coefficient of the cavity as:

$$\Gamma = \frac{L_m n}{L_m n + L_\alpha n_\alpha + \left[L-(L_m+L_\alpha)\right]} = \frac{L_m / v}{\frac{L_m}{v} + \frac{L_\alpha}{v_\alpha} + \frac{\left[L-(L_m+L_\alpha)\right]}{c}} \tag{27}$$

where $n = c/v$ and $n_\alpha = c/v_\alpha$ are the refractive index on the active medium and inside the absorber, respectively, L is the cavity length and L_α the saturable absorber length. Because $S_{S_{at}} = L_m(S)(\xi_2)$, Eq. (26) becomes then:

$$\frac{1}{\Gamma \mathrm{v}}\frac{dS}{dt}=\left(\sigma N+\frac{L_\alpha}{L_m}\sigma_\alpha N_\alpha\right)S-\left(\xi_1+\xi_2+\frac{L_\alpha}{L_m}\xi_\alpha\right)S. \tag{28}$$

This is the photon-flux equation inside a cavity with an active medium and a saturable absorber, as shown in Fig. 11.

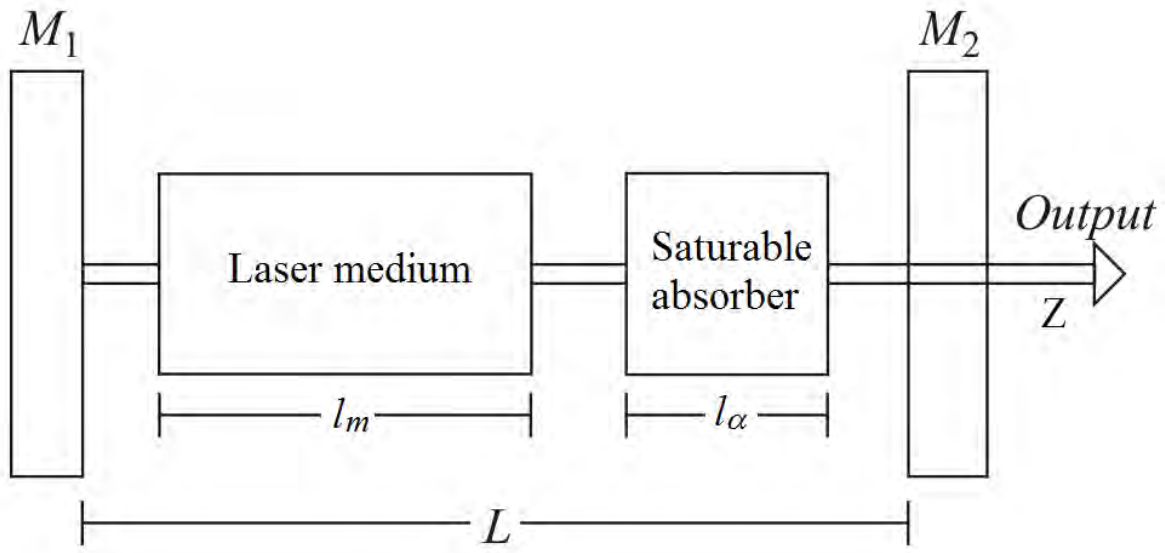

FIGURE 11. A laser cavity with an active medium and a saturable absorber.

Given that $k_\alpha=-\sigma_\alpha N_\alpha$ and defining T as the photons life-time inside a cavity with the form $T=\left[\Gamma\left(\xi_1+\xi_2+\frac{L_\alpha}{L_m}\xi_\alpha\right)\right]^{-1}$, Eq. (23) can be rewritten as:

$$\frac{dS}{dt}=\Gamma v\sigma NS-\Gamma v\frac{L_\alpha}{L_m}k_\alpha S-\frac{1}{T}S. \tag{29}$$

Therefore, for a complete description of a laser with saturable absorber, only three equations are needed: the photon-flux equation, an equation for the population inversion density on the active medium and the saturable population inversion equation that gives the saturation coefficient (taking into account $k_\alpha = -\sigma_\alpha N_\alpha$):

$$\begin{aligned}
\frac{dS}{dt} &= \Gamma v \sigma N S - \Gamma v \frac{L_\alpha}{L_m} k_\alpha S - \frac{1}{T} S, \\
\frac{dN}{dt} &= -\beta \frac{\sigma}{h\omega} N S + \frac{N_0 - N}{\tau}, \\
\frac{dk_\alpha}{dt} &= -\frac{2\sigma_\alpha k_\alpha S}{\hbar \omega} + \frac{k_{0\alpha} - k_\alpha}{\tau_\alpha}.
\end{aligned} \tag{30}$$

In order to have an easier handling [4] of the Eqs. (30) the next non-dimensional parameters are defined: $t' = t / \tau$, $G = \tau / T$, $\delta = \tau / \tau_\alpha$, $\rho = 2\sigma_\alpha / \beta\sigma$, $\alpha = \Gamma v \sigma T N$ and $\alpha_\alpha = -\Gamma v T k_{0\alpha} L_\alpha / L_m = -\Gamma v T \sigma_\alpha n_\alpha / L_m$; the new variables are: $n(t') = \Gamma v \sigma T N(t')$, $n_\alpha(t') = -\Gamma v T k_\alpha(t') L_\alpha / L_m$ and $m(t') = \beta B \tau S(t') / v = \beta \sigma \tau S(t') / h\omega$. With these new adimensional parameters and variables, the Eqs. (30) can be rewritten as:

$$\begin{aligned}
\frac{dm}{dt'} &= Gm\left(n + n_\alpha - 1\right), \\
\frac{dn}{dt'} &= \alpha - n\left(m + 1\right), \\
\frac{dn_\alpha}{dt'} &= \alpha_\alpha \sigma - n_\alpha \left(\rho m + \delta\right).
\end{aligned} \tag{31}$$

All the parameters used to define the saturable absorber are fixed, except for α_α, which includes a measure of the active centers absorbent density, for this reason, α_α will be used as the saturable absorber's identifying parameter.

The next step is to add an external modulation directly into the saturable absorber. The best way to do this is through its main parameter (i.e. α_α). Considering a CW low-energy laser which output is normalized and an EOM which responds linearly to the modulation injected energy (sinusoidal shape), Eqs. (31) are transformed into:

$$\begin{aligned}
\frac{dm}{dt'} &= Gm\left(n + n_\alpha - 1\right), \\
\frac{dn}{dt'} &= \alpha - n\left(m + 1\right), \\
\frac{dn_\alpha}{dt'} &= \sigma\alpha_\alpha\left[\frac{1+\cos\left(\omega_c t\right)}{2}\right] - n_\alpha\left(\rho m + \delta\right).
\end{aligned} \tag{32}$$

where ω_c stands for the modulation frequency applied to the EOM.

These three differential equations represent the working system, it must be noted that, in absence of modulation frequency applied to the EOM, ω, the system returns to Eqs. (31), i.e. rate equations for a laser with a passive saturable absorber.

2.3. LINEAR STABILITY ANALYSIS

Linear stability analysis (LSA) is used to understand the system dynamics [5]. The analysis is based on the linear disturbance equations, these equations are derived from the original equations. The method consists in linearizing the equations, obtain the initial state condition (i.e. when the derivatives are zero), expand the system about the initial state condition, construct the Jacobian matrix and find the eigenvectors and eigenvalues with the determinant equal to zero [6]. This gives as a result the fixed

points of the equations system, which must be analyzed in order to know what type of points are (i.e. fixed, source, saddle, etc.).

The equations of interest are Eqs. (32), these equations are non-autonomous due to the explicit time-dependence found in the cosine of the third equation. To be able to perform the LSA that dependence must be eliminated, to do that, a variable change must be applied, giving as a result, the next equations system:

$$\begin{aligned}
&\frac{dm}{dt'} = Gm\left(n + n_\alpha - 1\right), \\
&\frac{dn}{dt'} = \alpha - n\left(m + 1\right), \\
&\frac{dn_\alpha}{dt'} = \sigma\alpha_\alpha\left[\frac{1+\cos\left(x\right)}{2}\right] - n_\alpha\left(\rho m + \delta\right), \\
&\frac{dx}{dt} = \omega_c .
\end{aligned} \tag{33}$$

Naming the Eqs. (33) as:

$$\begin{aligned}
&f\left(m,n,n_\alpha,x\right) = \frac{dm}{dt'} = Gm\left(n + n_\alpha - 1\right), \\
&g\left(m,n,n_\alpha,x\right) = \frac{dn}{dt'} = \alpha - n\left(m + 1\right), \\
&h\left(m,n,n_\alpha,x\right) = \frac{dn_\alpha}{dt'} = \sigma\alpha_\alpha\left[\frac{1+\cos\left(x\right)}{2}\right] - n_\alpha\left(\rho m + \delta\right), \\
&j\left(m,n,n_\alpha,x\right) = \frac{dx}{dt} = \omega_c .
\end{aligned} \tag{34}$$

Supposing that $\left(m^*, n^*, n_\alpha{}^*, x^*\right)$ is the steady state, that is $f\left(m^*, n^*, n_\alpha{}^*, x^*\right) = 0$, $g\left(m^*, n^*, n_\alpha{}^*, x^*\right) = 0$, $g\left(m^*, n^*, n_\alpha{}^*, x^*\right) = 0$ and $j\left(m^*, n^*, n_\alpha{}^*, x^*\right) = 0$.

In order to know if the steady state is stable or unstable, a small perturbation (represented by the subscript "*p*") must be added to it

$$\begin{aligned} f &= f^* + f_p, \\ g &= g^* + g_p, \\ h &= h^* + h_p, \\ j &= j^* + j_p. \end{aligned} \tag{35}$$

with $\left(f_p, g_p, h_p, j_p\right) \ll 1$.

Now, the main question is: will the perturbations grow (steady state unstable) or decay (steady state stable)?

To be able to observe if the perturbations grow or decay, the perturbations derivatives must be found.

$$\begin{aligned} &\frac{df_p}{dt} = \frac{dm}{dt} = f(m,n,n_\alpha,x) = f(m^* + f_p, n^* + g_p, n_\alpha{}^* + h_p, x^* + j_p) = \\ &f(m^*,n^*,n_\alpha{}^*,x^*) + \frac{\delta}{\delta m} f(m^*,n^*,n_\alpha{}^*,x^*) f_p + \frac{\delta}{\delta n} f(m^*,n^*,n_\alpha{}^*,x^*) g_p + \\ &\frac{\delta}{\delta n_\alpha} f(m^*,n^*,n_\alpha{}^*,x^*) h_p + \frac{\delta}{\delta x} f(m^*,n^*,n_\alpha{}^*,x^*) j_p + \text{high order terms} \end{aligned} \tag{36}$$

Following the Taylor series expansion shown in Eqs. (36) the derivatives for each perturbation are:

$$\begin{aligned}
\frac{df_p}{dt} &= \frac{\delta}{\delta m} f.f_p + \frac{\delta}{\delta n} f.g_p + \frac{\delta}{\delta n_\alpha} f.h_p + \frac{\delta}{\delta x} f.j_p, \\
\frac{dg_p}{dt} &= \frac{\delta}{\delta m} g.f_p + \frac{\delta}{\delta n} g.g_p + \frac{\delta}{\delta n_\alpha} g.h_p + \frac{\delta}{\delta x} g.j_p, \\
\frac{dh_p}{dt} &= \frac{\delta}{\delta m} h.f_p + \frac{\delta}{\delta n} h.g_p + \frac{\delta}{\delta n_\alpha} h.h_p + \frac{\delta}{\delta x} h.j_p, \\
\frac{dj_p}{dt} &= \frac{\delta}{\delta m} j.f_p + \frac{\delta}{\delta n} j.g_p + \frac{\delta}{\delta n_\alpha} j.h_p + \frac{\delta}{\delta x} j.j_p,
\end{aligned} \tag{37}$$

The system presented in Eqs. (37) can be rewritten in the matrix form:

$$\begin{pmatrix} f_p' \\ g_p' \\ h_p' \\ j_p' \end{pmatrix} = \begin{pmatrix} \frac{\delta}{\delta m} f & \frac{\delta}{\delta n} f & \frac{\delta}{\delta n_\alpha} f & \frac{\delta}{\delta x} f \\ \frac{\delta}{\delta m} g & \frac{\delta}{\delta n} g & \frac{\delta}{\delta n_\alpha} g & \frac{\delta}{\delta x} g \\ \frac{\delta}{\delta m} h & \frac{\delta}{\delta n} h & \frac{\delta}{\delta n_\alpha} h & \frac{\delta}{\delta x} j \\ \frac{\delta}{\delta m} j & \frac{\delta}{\delta n} j & \frac{\delta}{\delta n_\alpha} j & \frac{\delta}{\delta x} h \end{pmatrix} \begin{pmatrix} f_p \\ g_p \\ h_p \\ j_p \end{pmatrix} = \Im \begin{pmatrix} f_p \\ g_p \\ h_p \\ j_p \end{pmatrix}, \tag{38}$$

where $\Im$ denotes the Jacobian matrix of the original system at the steady state.

Substituting the values in the Jacobian function and the next matrix is obtained:

$$\begin{pmatrix} G\left(n+n_\alpha-1\right) & Gm & Gm & 0 \\ -n & -m-1 & 0 & 0 \\ -\rho n_\alpha & 0 & -\rho m-\delta & -\frac{\delta\alpha_\alpha}{2}\sin(x) \\ 0 & 0 & 0 & 0 \end{pmatrix}. \tag{39}$$

The next step is to find the eigenvectors and eigenvalues of the system $(\Im - \lambda I)\partial_p = 0,$ so the determinant would be:

$$\left|\Im - \lambda I\right| = 0. \tag{40}$$

The matrix for the former equation is:

$$\begin{pmatrix} G(n+n_\alpha - 1) - \lambda & Gm & Gm & 0 \\ -n & -m-1-\lambda & 0 & 0 \\ -\rho n_\alpha & 0 & -\rho m - \delta - \lambda & -\frac{\delta \alpha_\alpha}{2}\sin(x) \\ 0 & 0 & 0 & -\lambda \end{pmatrix} = 0, \tag{41}$$

The solutions for the perturbed steady-state of the original system are:

$$\begin{aligned} m^s &= 0, \\ n^s &= \alpha, \\ {n_\alpha}^s &= \alpha_\alpha, \\ x^s &= 0. \end{aligned} \tag{42}$$

Substituting the former solutions in Eqs. (41), the matrix transforms into:

$$\begin{pmatrix} G(\alpha + \alpha_\alpha - 1) - \lambda & 0 & 0 & 0 \\ -\alpha & -1-\lambda & 0 & 0 \\ -\rho\alpha_\alpha & 0 & -\delta - \lambda & 0 \\ 0 & 0 & 0 & -\lambda \end{pmatrix} = 0, \tag{43}$$

Matrix (43) has the next characteristic equation:

$$\left[G(\alpha + \alpha_\alpha - 1) - \lambda\right][-1-\lambda][-\delta - \lambda][-\lambda] = 0, \tag{44}$$

where $\lambda_1 = G(\alpha + \alpha_\alpha - 1)$, $\lambda_2 = -1$, $\lambda_3 = -\delta$ and $\lambda_4 = 0$ are eigenvalues which are all real; being λ_2 and λ_3 always negative (i.e. the perturbation will decay) and λ_4 is critically stable. Therefore, the stability condition is defined only by the sign of λ_1, i.e. the fixed point is a source when $\alpha_\alpha + \alpha > 1$ as shown in Fig. 12.

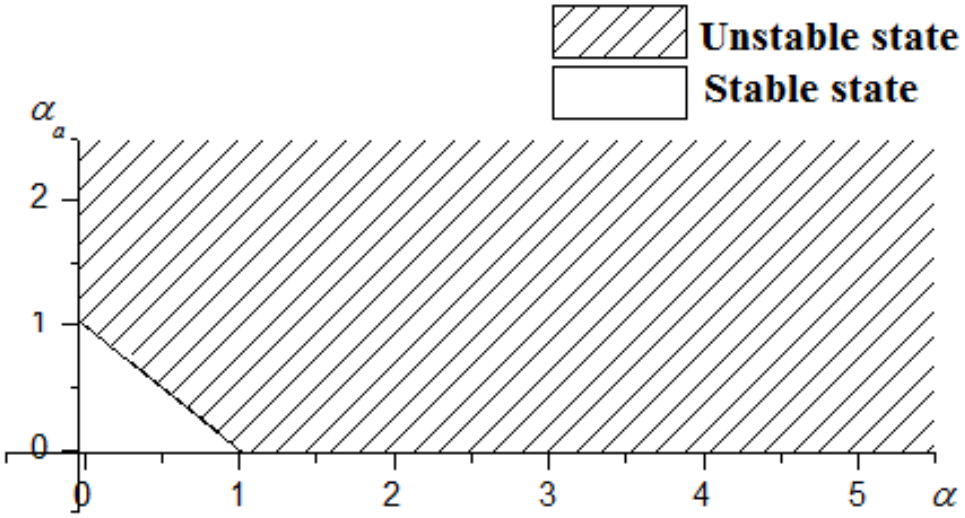

FIGURE 12. Stability condition given by the relation between α and α_α.

SECOND CHAPTER REFERENCES

1. H. Statz, and G. De Mars, "Transients and Oscillation Pulses in Masers". Quantum Electronics, 530-537 (1960).

2. L. Tarassov, *Physique des processus dans les générateurs de rayonnement optique cohérent* (Éditons MIR, 1981).

3. C.L. Tang, H. Statz and G. de Mars, "Spectral output and spiking behavior of solid-state lasers", J. Appl. Phys. **34,** 2289-2295 (1963).

4. M. Braun, *Differential equations and their applications: An introduction to applied mathematics* (Springer, 1992).

5. L. C. Haber, *Investigation of dynamics in turbulent swirling flows aided by linear stability analysis*, Ph. D. Thesis (Virginia Polytechnic Institute, 2003)

6. R. S. Palais, *An introduction to wave equations and solitons* (Chinese Academy of Sciences, 2000).

7. L. W. Hilman, *Dye laser principles* (Academic press, 1990).

8. R. Paschotta, *Encyclopedia of laser physics and technology* (Wiley, 2008).

9. A. C. Newell and J. V. Moloney, *Nonlinear Optics* (Addison-Wesley Publishing Co., 1992).

10. E. Infeld and R. Rowlands, *Nonlinear Waves, Solitons and Chaos* (Cambridge University Press, Cambridge, 1990).

11. V. Aboites, K. J. Baldwin, G. J. Crofts, and M. J. Damzen, "Dye High Power optical Switch", Rev. Mex. Fis. **39** (4), 581 (1993).

12. C. E. Preda, B. Ségard, and P. Glorieux, "Comparison of laser models via laser dynamics: The example of the Nd^{3+}:YVO_4 laser", Opt. Commun. **261**(1), 141-148 (2006).

CHAPTER 3

RESULTS AND CONCLUSIONS

3.0. INTRODUCTION

In this chapter the representing equations for the proposed experiment are numerically solved in order to study the system dynamics. In some explored regions the cnoidal waves are observed, the numerics were performed for different control parameters.

3.1. CONTROLLING THE SYSTEM DYNAMICS

To find the solutions of the Eqs. (32) a program was build using the typical Statz – de Mars parameters for a Dye laser [1,2] $G = 200$, $\alpha = 4$, $\delta = 1$ and $\rho = 0.001$ and using as initial condition a neighboring point to a system's stable fixed point [3], i.e. $m_0 = 0.25$, $n_0 = 0$ and $n_{\alpha 0} = 0.152$, that corresponds to a non-stationary fixed point neighboring.

As expected, when the modulation is not applied to the SA, the system tends to a fixed point in a small computational time, as shown in Fig. 13. Once the modulation is applied, the system starts to change into a periodic one as can be observed in Fig. 14.

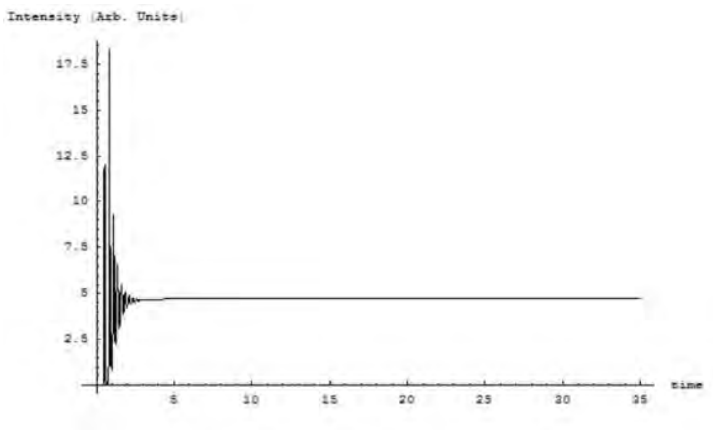

FIGURE 13. Laser output without external modulation, the system tends to a fixed point.

With a fixed modulation, the only parameter we can manipulate is α_α, a measure of the active centers absorbent density contained in the SA. Since all the geometrical values involved in the definition of α_α are fixed, the parameter α_α will be identified as an absorption ratio and therefore will depend on the chosen SA (in a dye SA its dependence vary according to the dye concentration). For this numerical experiment, its value was chosen in a practical range (between 0.3 and 60).

If all the physical parameters involved in this experiment are fixed, the available variables are only the external modulation, represented by ω_c, and the absorption ratio, represented by α_α. Due to this reason, the experiment is segmented in two parts. The first one is realized with a fixed modulation frequency and varying absorption ratio, and the second one is the reverse case, i.e. with fixed absorption ratio and varying modulation frequency.

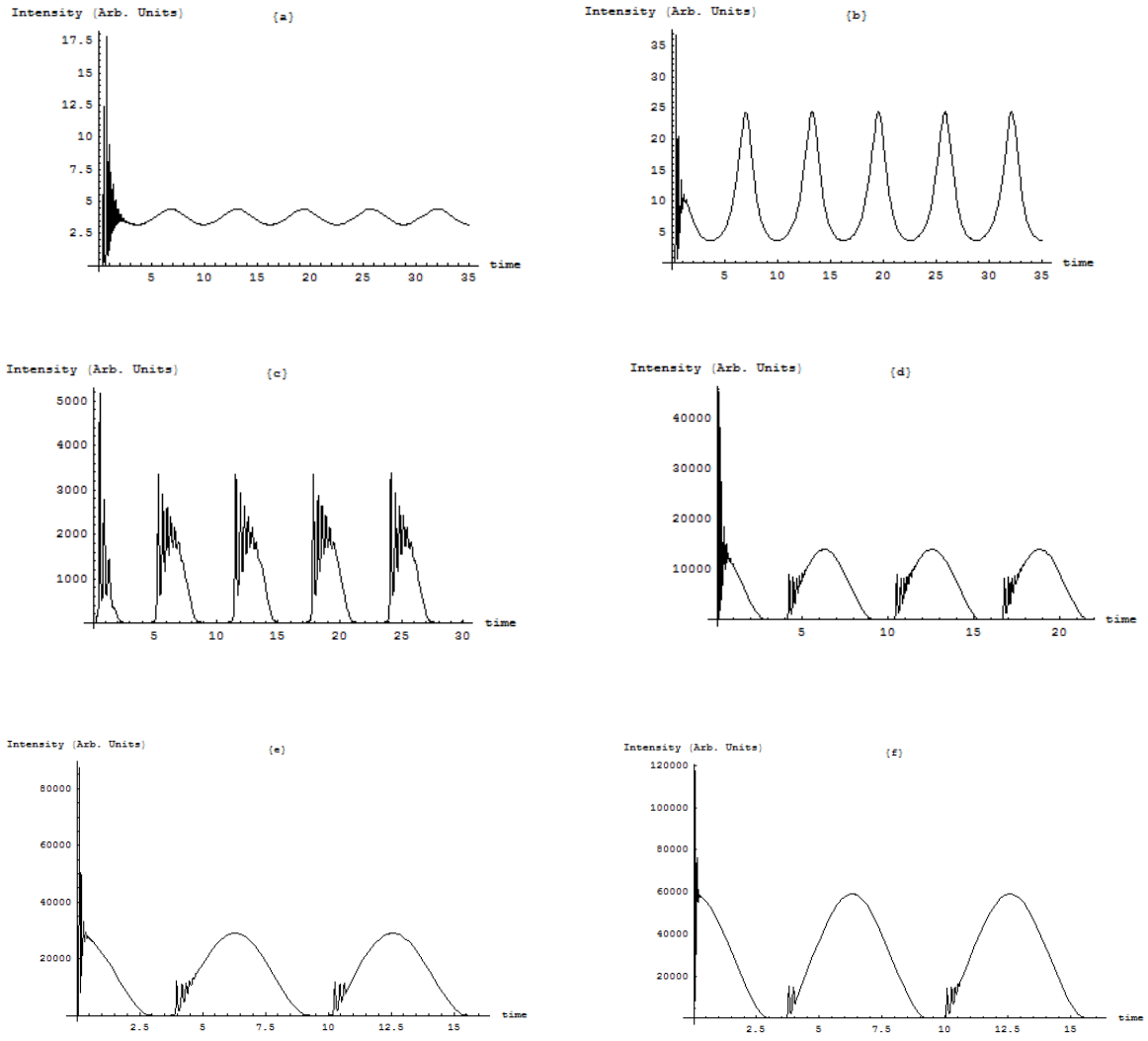

FIGURE 14. Laser output with fixed modulation ($\omega_c = 1$) and variable absorption ratio.

a) $\alpha_\alpha = 0.3$, b) $\alpha_\alpha = 1$, c) $\alpha_\alpha = 3$, d) $\alpha_\alpha = 15$, e) $\alpha_\alpha = 30$ and f) $\alpha_\alpha = 60$.

For the first case, when the Eqs. (32) were solved without modulation, the output photon-flux, m, reached a fixed point in few iterations no matter the absorption ratio used (transients), Fig. 13, as soon as the modulation is injected into the SA a periodic train begins to appear with α_α as small as 0.3, Fig. 14(a), as α_α is increased the maximum intensity reached increases and a region of different frequencies coexistence

(undamped undulations) begins to appear at a certain location in the pulse, the localization of this region depends on the absorption ratio.

It can be observed from Fig. 13 that the laser output tends to a fixed point when the SA is in passive configuration, *i.e.* without external modulation; as soon as the SA is turned into an active device (Fig. 14), different packages of pulses are obtained depending on the SA's absorption ratio (α_a), the bigger the concentration the higher the reached intensity. The laser output, in this case, goes from a continuous wave regime to a high-intensity peaks train passing, through an undamped undulations window moving across the pulse's body.

When the absorption ratio is larger than a threshold that depends on the modulation frequency, the phase diagram between m and n_a exhibits instead of one, two critical points, as shown in figure 15. When the frequency is normalized with the laser's relaxation frequency this phenomenon appears for an α_a value near 1.4. If $\alpha_a = 30$ the two critical points are separated in the phase space diagrams (figure 15(b)).

Being in the fixed point without modulation, the laser represents periodic oscillations when the external modulation is applied and undergoes the period-doubling bifurcation when the modulation frequency is increased.

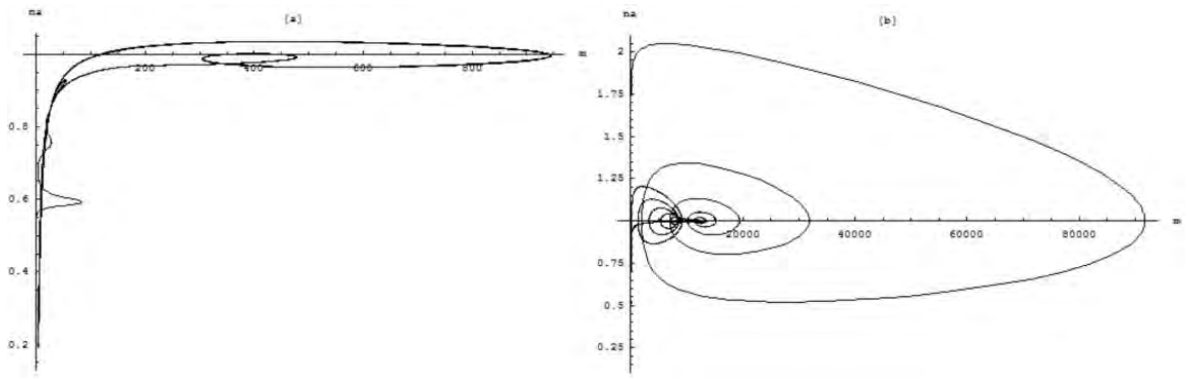

FIGURE 15. Phase diagram m vs n_a. a) with $\alpha_a = 1.4$ b)with $\alpha_a = 30$.

For the second case (i.e. fixed absorption ratio), a comprehensive study on the output signal in terms of ω_c was done for an $\alpha_a = 15$, the value was chosen first of all because the undamped undulations are obvious for small ω_c and are nowhere near the maximum intensity reached by the laser output; its behavior is representative of what happens at any frequency even if there are some differences in detail.

Figure 16 shows how the signal frequency increases following the change in the modulation frequency. As the frequency rises, a threshold is obtained where the narrow pulse train is reached, its value is closely related with α_a, a change in the absorption ratio only moves the undamped undulations window; the window is shifted towards the right (both thresholds get larger) as α_a is increased. The second threshold corresponds to the appearance of a narrow pulse train, when $\alpha_a = 15$ the narrow high intensity pulse train is obtained at around $\omega_c = 35$.

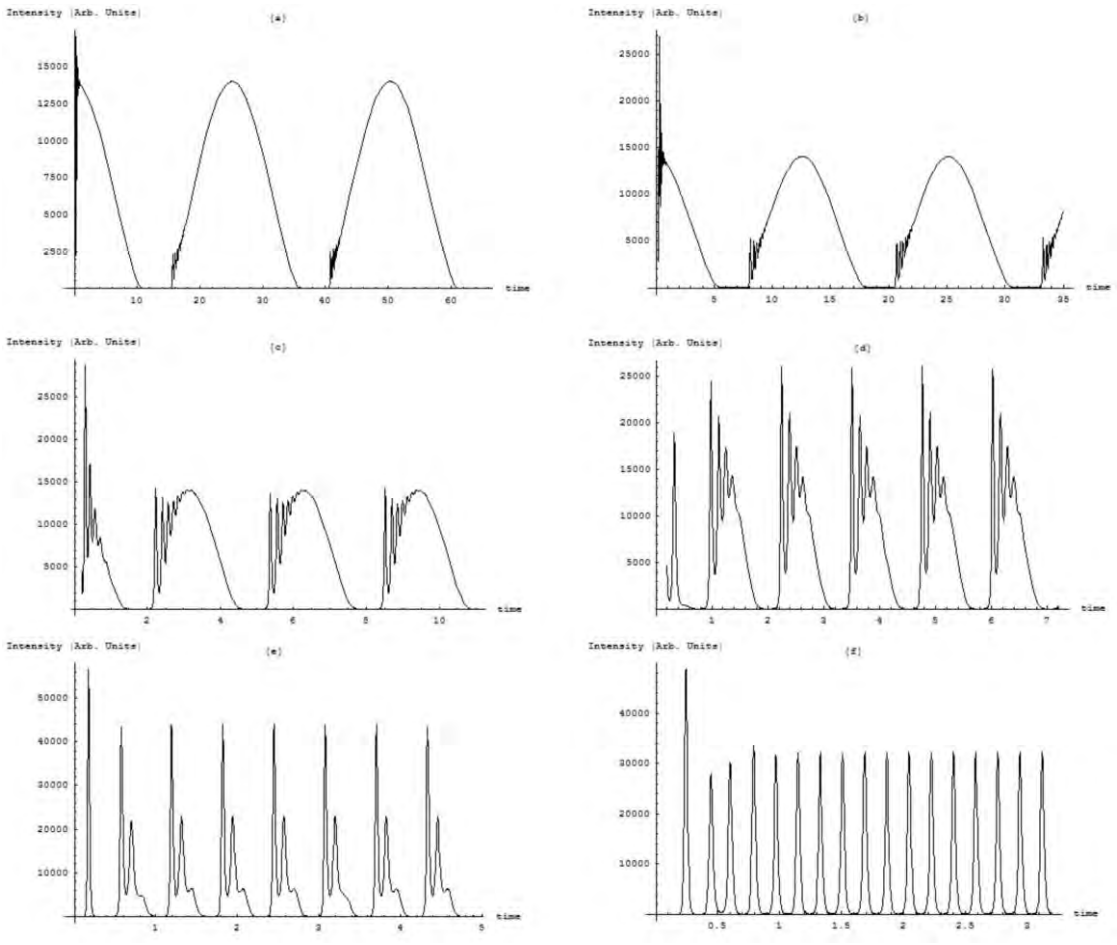

FIGURE 16. Pulse shape at $\alpha_a = 15$ with different frequencies a) $\omega_c = 1/4$, b) $\omega_c = 1/2$, c) $\omega_c = 2$, d) $\omega_c = 5$, e) $\omega_c = 10$, f) $\omega_c = 35$.

The dependence between the output pulse width and the modulation frequency, shown in Fig. 17, is clearly a very good approximation to an exponential decay. It must be noted that the modulation frequency ω_c enters the equation as an integer multiple of the laser relaxation frequency ω, so that the pulse duration is calculated from the relaxation time. From the above considerations one can observe a width lower limit around 19 ns achieved approximately at 80 KHz, which is 35 times the relaxation frequency.

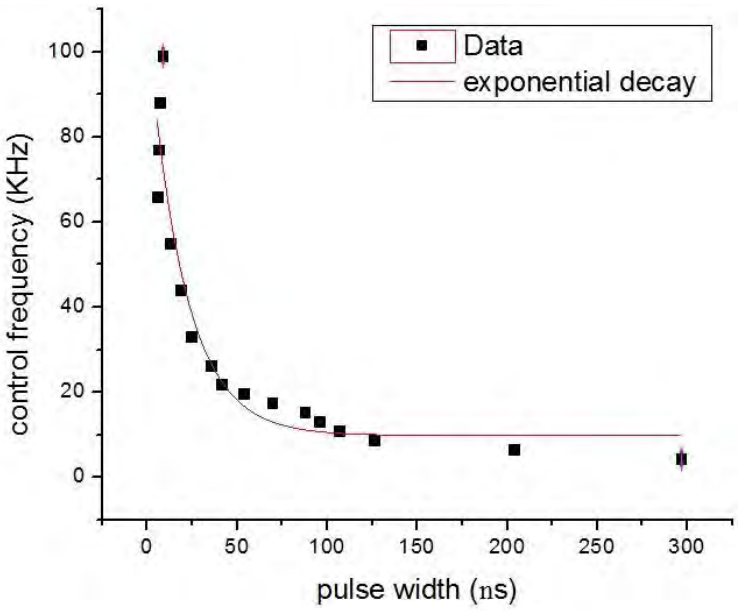

FIGURE 17. Pulse width against control frequency. It is shown how the pulses width become narrower as the control frequency is increased.

3.2. CNOIDAL WAVE OBSERVATION

Figure 18 shows the temporal dynamics of the laser output for fixed α_a = 15 and different modulation frequencies ω_c. For small ω_c (lower than the laser relaxation oscillation frequency), the laser generates pulse trains with localized undulation windows, which are the damped relaxation oscillations (Figs. 18(a)--18(c)). For higher ω_c, only one frequency remains, i.e. the laser oscillates with the modulation frequency (Figs. 18(d)--18(f)), and the pulse shape strongly depends on ω_c. One important aspect is that as ω_c is increased; the peak amplitude first increases, reaches a maximum, and then decreases, thus going from a $sech^2$ (when the amplitude is maximum, Fig. 18(d)) to almost harmonic oscillations (Fig. 18(f)). While the peak amplitude is decreasing, the laser intensity never falls down to zero again; the continuous background appears

because the frequency applied to the SA is so high that it has not enough time, neither to relax to its ground state nor to saturate. As ω_c further increases, the signal behavior becomes more and more sinusoidal with relatively small amplitude. We repeat the simulations for different α_a with a step of 5 and find that the results shown in Fig. 18 for $\alpha_a = 15$ follow exactly the same qualitative pattern for any other $\alpha_a \in [5, 60]$.

In 2004, Y. Kartashov et al [4,5] demonstrated that certain cnoidal waves can be forced to stabilized (this because normally the cnoidal waves are unstable), that forced-stable waves were bounded, as in this case, by two values of control parameter; in the case presented here, the boundaries are given by the modulation frequency.

It must be noted that the cnoidal waves obtained through the presented scheme are founded in the inverse expected order, first, the upper limit was achieved (the soliton shape) and, second the sinusoidal shape (the cosine limit).

The obtained pulse trains are asymptotically stable due to the quadratic non-linearities given by the SA.

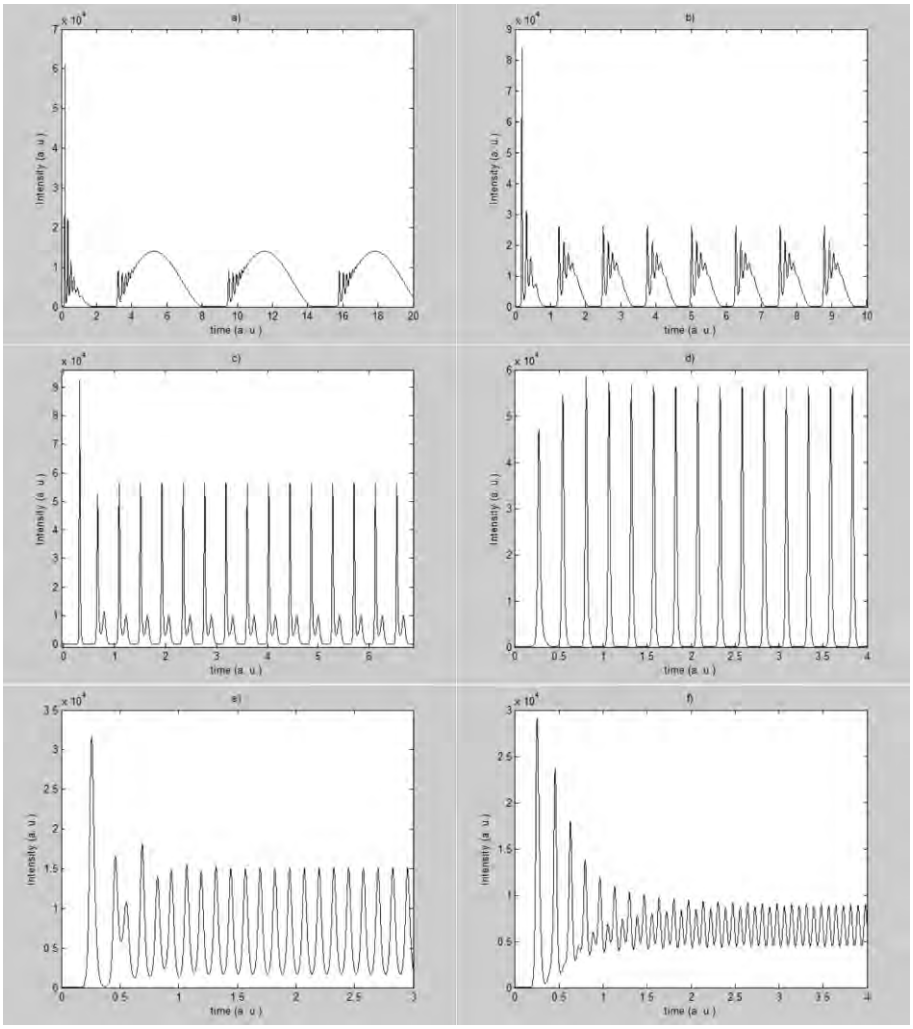

FIGURE 18. Laser output intensity for α_a = 15 and control frequencies (a) ω_c = 1, (b) 5, (c) 15, (d) 25, (e) 50, and (f) 75.

Another interesting feature of the observed dynamics is that when the pulse train amplitude reaches its maximum, a $sech^2$ (soliton-like) shape approximates the pulse shape with a very good precision as demonstrated in Fig. 19. This is confirmed by overlapping one pulse with a $sech^2$ waveform; the difference that appears on the base right hand side is very small (in the order of 2%, and always less than 5%). We find that for every saturable absorber coefficient α_a there is an optimal modulation frequency ω_s

for which this soliton-shape approximation has better precision than for other frequencies.

As seen from Fig. 20, ω_s increases approximately linearly with α_a with two jumps at α_a = 5 and α_a = 30. We should note that several theoretical and experimental works report the existence of solitons meaning that the pulses shape obtained at the output presents the soliton characteristic functions (*sech* and $sech^2$). While in the cited works, the difference between the reported pulses and the soliton shape is larger than 5%; our system allows the soliton generation with a higher precision, which makes it prominent for optical communication purposes.

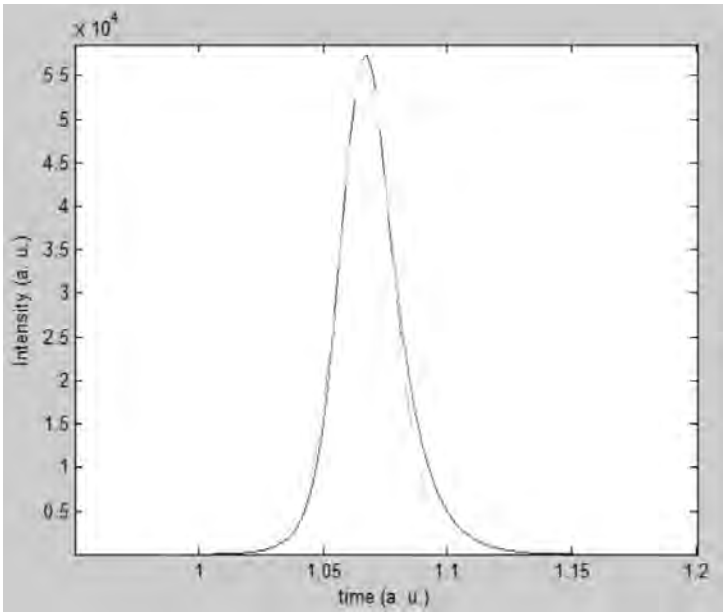

FIGURE 19. Overlapping of one pulse taken at α_a = 15 and ω_c = 25 (solid line) with a $sech^2$ wave form (dashed line).

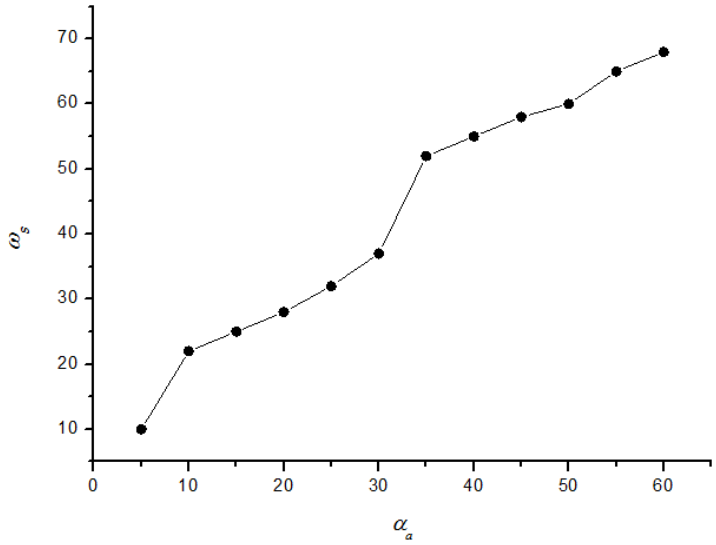

FIGURE 20. Modulation frequency ω_s and absorption ratio of saturable absorber corresponding to soliton-shape pulses.

3.3. CONCLUSIONS

This work effectively shows how a saturable absorber can be made in to an *active* device to control the output of a laser.

The insertion of a modulated signal directly into the saturable absorber modifies the continuous output driving it into a periodic one. The larger the α_a the higher the laser intensity obtained, and the more comb-like it becomes. For a given α_a there are two important thresholds: the modulation frequency where the undamped undulations appear and the one where they disappear, as the absorption ratio is increased, the undulations window is shifted towards higher frequencies.

For a given α_a, as the modulation frequency is increased, the output signal changes from a smooth periodic function to a clear comb-like pulse train whose width decreases exponentially, thus the saturable absorber is behaving as an *active* device.

It was also demonstrated with a rate equations model (based on SdM) that a laser with an active saturable absorber under the influence of a control radiation from another laser can generate cnoidal waves within a certain range of control parameters, which bound soliton-like and sinusoidal regimes.

No matter the physical saturable absorber characteristics, there is always a certain value of the modulation frequency that would result in the cnoidal waves generation.

When we compared the resulting pulses with a typical soliton shape ($sech^2$), we obtained less than 5% error at the pulse base. The proposed system can be a base for building a reliable and cheap device to generate cnoidal waves as efficient information carriers for optical communication; the proposed system is economic due to the elements involved, at using general purpose laser elements and not ultra-fast optics elements, the experimental implementation of the presented scheme results less expensive.

3.4. FUTURE WORK

In this thesis the studies were done with a simple rate-equations model, we believe that the obtained results can be applied to different laser systems (e.g. Erbium-doped fiber laser) and not only to Dye lasers.

As part of the future work, a more complete model will be studied theoretically and experimentally.

The following experiment was implemented as a preliminary experimental attempt:

A 1550-nm EDFL diode pumped at 980-nm was used; the experimental array is shown in Fig. 21. A 4-m Fabry-Perot laser cavity was formed by an active heavily doped 90-

cm-long erbium fiber, a Faraday rotating mirror (FRM) and a fiber Bragg grating (FBG) with a 100-pm FWHM bandwidth, having, respectively, 100% and 98% reflectivities. FRM was used in order to avoid polarization mode beating. An electro-optical modulator (EOM), modulated through a functions generator, was placed inside the cavity. The fiber output, after passing through a wavelength-division multiplexer (WDM) was recorded with a photodetector and analyzed with an oscilloscope. The pump-diode current was fixed at 64 mA, which results in a pump power of 15.5 mW. This corresponds to about 10% over the laser threshold of 14 mW. This value was chosen in order to obtain CW laser operation. The EDFL's relaxation frequency is around 28 kHz due to the applied pump power.

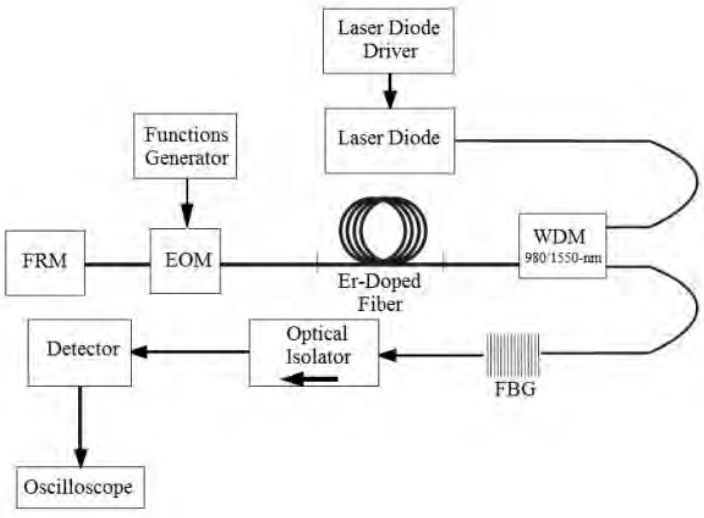

FIGURE 21. Experimental set-up implemented for search cnoidal waves.

Figure 22 shows preliminary results obtained for the shown configuration, these pulses are generated when the frequency applied to the EOM is around 9.1 MHz, which correspond to 325 times the laser's relaxation frequency. It is expected that if the

erbium-doped fiber length changes, the frequency needed to generate cnoidal waves would be shifted, if the length is reduced, so the frequency would be diminished and conversely.

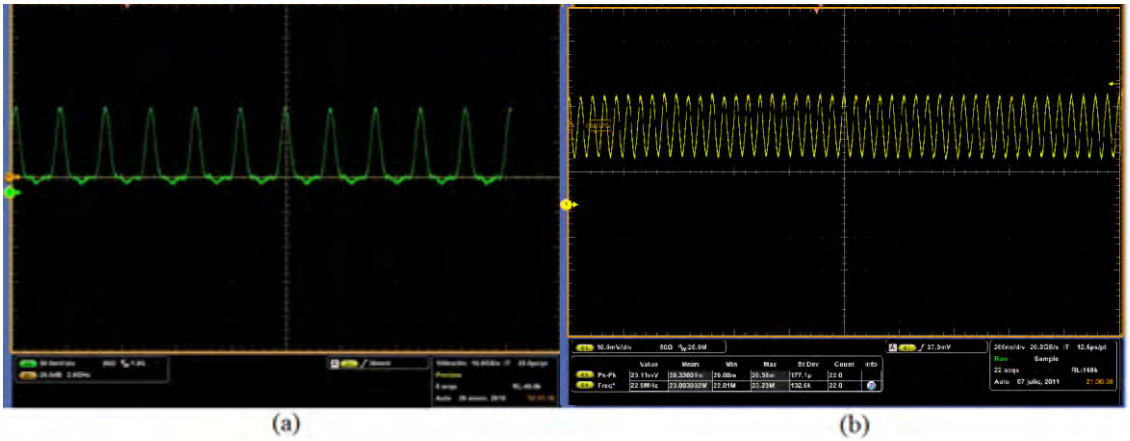

FIGURE 22. Experimental cnoidal wave limits. a) soliton-shape limit, b) sinusoidal shape limit.

It is important to complete the experimental part of this work in order to be able to construct a cheap cnoidal wave generator that can be reliable used with optical communications purposes.

THIRD CHAPTER REFERENCES

1. M. J. Damzen, K. J. Baldwin, and P. J. Soan, "Optical switching and high-resolution image transfer in a saturable dye spatial light modulator" J. Opt. Soc. Am. B **11**, 313 - 319 (1994).

2. L. W. Hilman, *Dye laser principles* (Academic press, 1990).

3. V. Aboites, K. J. Baldwin, G. J. Crofts, and M. J. Damzen, "Fast high power optical switch", Opt. Comm. **98**, 298 - 302 (1993).

4. Y. A. Kartashov, A. A. Egorov, A. S. Zelenina, V. A. Vysloukh and L. Torner, "Stabilization of one-dimensional periodic waves by saturation of the nonlinear response", Phys. Rev. E **68**, 065605(R) (2003).

5. Y. A. Kartashov, A. A. Egorov, A. S. Zelenina, V. A. Vysloukh and L. Torner, "Stable multicolor periodic-wave arrays", Phys. Rev. Lett. **92**(3) (2004).

6. P. G. Drazin and R. S. Johnson, *Solitons: An introduction*. *2nd ed*. (Cambridge University Press, 1989).

7. N. Akhmediev and A. Ankiewicz, *Solitons Nonlinear Pulses and Beams* (Chapman & Hall, 1997).

8. L. Tarassov, *Physique des Processus dans les Générateurs de Rayonnement Optique Cohérent* (Éditons MIR, 1981).

9. P. P. Sorokin and J. R. Lankard, "Stimulated emission observed from an organic dye chloro-aluminum phthalocyanine" IBM J. Res. Develop. **10**, 162-3 (1966).

10. B. K. Garside and T. K. Lim, "Laser mode locking using saturable absorbers", J. Appl. Phys. **44** (5), 2335 (1973).

11. W. Dietel, E.Döpel and D. Kühlke, "Passive mode locking of an argon laser using rhodamine 6G saturable absorber and double mode locking of the pump and dye laser system", Sov. J. Quantum Electron. **12**, 668 (1982)

12. V. V. Nevdakh, O. L. Gaiko, L. N. Orlov, “New operation regimes of a CO_2 laser with intracavity saturable absorber”, Opt. Comm. **127**, 303 - 306 (1996).

13. A. N. Pisarchik, A. V. Kir'yanov, Y. O. Barmenkov, and R. Jaimes-Reátegui, "Dynamics of an erbium-doped fiber laser with pump modulation: theory and experiment," J. Opt. Soc. Am. B **22**, 2107-2114 (2005).

14. M. E. Fermann, “Passive mode locking by using nonlinear polarization evolution in a polarization-maintaining erbium-doped fiber”, Opt. Lett. 18 (11), 894 (1993).

15. Schmidt *et al.*, “Passive mode locking of Yb:KLuW using a single-walled carbon nanotube saturable absorber”, Opt. Lett. 33 (7), 729 (2008).

16. W. Dietel et al*.,* “Passive mode locking of an argon laser using rhodamine 6G saturable absorber and double mode locking of the pump and dye laser system” Sov. J. Quantum Electron**, 12** (5), 668 (1982).

17. N. J. Zabusky and M. D. Kruskal, “Interaction of 'Solitons' in a collisionless plasma and the recurrence of initial states”, Phys. Rev. Lett. **15**, 240-243 (1965).

18. J. E. Bjorkholm and A. A. Ashkin, “Cw self-focusing and self-trapping of light in sodium vapor”, Phys. Rev. Lett. **32**, 129-132 (1974).

19. F. Gèrôme, P. Dupriez, J. Clowes, J. C. Knight and W. J. Wadsworth, “High power tunable femtosecond soliton source using hollow-core photonic bandgap fiber, and its use for frequency doubling”, Opt. Express **16**, 2381-2386 (2008).

20. R. Herda and O. G. Okhotnikov, "All-fiber soliton source tunable over 500 nm", in Conference on Lasers and Electro-Optics/Quantum Electronics and Laser Science and Photonic Applications Systems Technologies, Technical Digest (CD) (Optical Society of America, 2005), paper JWB39.

21. S. Chouli and P. Grelu, "Rains of solitons in a fiber laser", Opt. Express **17**, 11776-11781 (2009).

22. J. Li, X. Liang, J. He, L. Zheng, Z. Zhao and J. Xu, "Diode pumped passively mode-locked Yb:SSO laser with 2.3ps duration", Opt. Express **18**, 18354-18359 (2010).

23. M. G. Clerc, S. Coulibaly, N. Mujica, R. Navarro and T. Sauma, "Soliton pair interaction law in parametrically driven Newtonian fluid", Phil. Trans. R. Soc. A **367**, 3213-3226 (2009).

24. J. M. Saucedo-Solorio, A. N. Pisarchik, A. V. Kir'yanov, and V. Aboites, "Generalized multistability in a fiber laser with modulated losses," J. Opt. Soc. Am. B **20**, 490-496 (2003).

25. A. N. Pisarchik, Y. O. Barmenkov, and A. V. Kir'yanov, "Experimental characterization of the bifurcation structure in an erbium-doped fiber laser with pump modulation," IEEE J. Quantum Electron. **39**, 1567-1571 (2003).

26. L. H. Zao, and C. Q. Dai, "Self-similar cnoidal and solitary wave solutions of the (1+1)-dimensional generalized nonlinear Schrödinger equation," Eur. Phys. J. D **58**, 327-332 (2010).

27. V. M. Petnikova, V. V. Shuvalov and V. A. Vysloukh, "Multicomponent photorefractive cnoidal waves: Stability, localization, and soliton asymptotics," Phys. Rev. E. **60,** 1009-1018 (1999).

28. A. N. Pisarchik, A. V. Kir'yanov, Y. O. Barmenkov, and R. Jaimes-Reátegui, "Dynamics of an erbium-doped fiber laser with pump modulation: theory and experiment," J. Opt. Soc. Am. B **22**, 2107-2114 (2005).

APPENDIX A

LIST OF PUBLICATIONS

A1.1. PEER-REVIEWED INDEXED JOURNALS

1. V. aboites, and **M. Wilson**, "Tinkerbell chaos in a ring phase-conjugated resonator", Int. J. Pure Appl. Math. **54**(3), 429-435 (2009).
2. **M. Wilson**, and M. Huicochea, "Duffing chaotic laser resonator", Iraqui J. Appl. Phys. **1**(5), 236-240 (2009).
3. **M. Wilson**, and M. Huicochea, "Driving a ring resonator's dynamics into chaos", Int. J. Pure Appl. Math. **60**(3), 239-245 (2010).
4. **M. Wilson**, V. Aboites, A. N. Pisarchik, V. Pinto, and Y. O. Barmenkov, "Controlling a laser output through an active saturable absorber", Rev. Mex. Fis. 57(3), 250-254 (2011).
5. **M. Wilson**, V. Aboites, A. N. Pisarchik, V. Pinto, and M. Taki, "Generation of cnoidal waves by a laser system with a controllable saturable absorber", Opt. Express **19**(15), 14210-14216 (2011).

A1.2. CONFERENCES

1. **M. Wilson**, and V. Aboites, "Stability and chaos in a laser with an intracavity saturable absorber", Fourth international conference of pure and applied mathematics, Plovdiv, Bulgaria (2007).
2. **M. Wilson**, "Photonic crystal fibers: uses and applications", Sixth national symposium of electronics and electro-mechanics" Los Mochis, Mexico (2008).
3. **M. Wilson**, and V. Aboites, "Resonador laser caótico de Duffing" LII Physics National Conference, Acapulco, Mexico (2009).
4. D. Dignowity, V. Aboites, **M. Wilson**, and M. Huicochea, "Control de la dinámica especial de un resonador láser" LII Physics National Conference, Acapulco, Mexico (2009).
5. **M. Wilson**, V. Aboites, and A. N. Pisarchik, "Sincronización de una red de láseres logísticos" XXIII Optics Anual Meeting, Puebla, Mexico (2010).
6. **M. Wilson**, V. Aboites, and A. N. Pisarchik, "Solitons formation in a laser with an active saturable absorber" Mexican Conference of Complexity Sciences, Mexico City, Mexico (2010).
7. **M. Wilson**, and V. Aboites, "Synchronization in a Gaussian lasers network" Mexican Conference of Complexity Sciences, Mexico City, Mexico (2010).
8. **M. Wilson**, and V. Aboites, "Optical resonators and dynamic maps" 22th International Conference of Optics, Puebla, Mexico (2011).